UNIVERSIDADE
NOVA
DE LISBOA

CHARACTERIZATION OF THE MAJOR AUTOLYSIN IN *STAPHYLOCOCCUS AUREUS*

JOANA FILIPA GOMES DA SILVA

DISSERTATION PRESENTED TO OBTAIN A MASTER DEGREE IN MEDICAL MICROBIOLOGY

OCTOBER 2015

CHARACTERIZATION OF THE MAJOR AUTOLYSIN IN *STAPHYLOCOCCUS AUREUS*

JOANA FILIPA GOMES DA SILVA

DISSERTATION PRESENTED TO OBTAIN A MASTER DEGREE IN MEDICAL MICROBIOLOGY

Supervisor: Dr. Rita Sobral, UCIBIO-FCT/UNL

Co-supervisor: Prof. Ana Madalena Ludovice, DCV-FCT/UNL; ITQB/UNL

OCTOBER 2015

Bibliographic elements resulting from this dissertation

Silva, J., I. Grilo, A. M. Ludovice, H. de Lencastre, R. G. Sobral. Characterization of the major peptidoglycan hydrolase of *Staphylococcus aureus*. MicroBiotec'15 – Portuguese Congress of Microbiology and Biotechnology 2015. P230, pg. 354. December 10-12, 2015.

Agradecimentos

À Doutora Rita Sobral, expresso o meu profundo agradecimento pela orientação, pela disponibilidade para o debate de ideias e apoio que muito elevaram os meus conhecimentos científicos e, sem dúvida, muito estimularam o meu desejo de querer saber mais e a vontade constante de querer fazer melhor.

Agradeço, também, à Professora Ana Madalena Ludovice, pela co-orientação neste projeto. Muito obrigada pelo profissionalismo e pela total disponibilidade que sempre revelou para comigo.

Aos meus colegas de laboratório, Bárbara, Raquel, Ricardo e Vanessa, um muito obrigado pela vossa amizade, companheirismo e ajuda, fatores muito importantes na realização desta tese e que me permitiram que cada dia fosse encarado com um sorriso e particular motivação.

À Inês Grilo, com quem tive o privilégio de colaborar, agradeço toda a disponibilidade e paciência que teve para comigo nas semanas que estive no ITQB/UNL.

Aos colegas do UCIBIO, quero agradecer a disponibilidade para partilha de ideias, pelo auxílio e pelos momentos que relembro com um sorriso nos lábios, em particular à Cynthia Barroco, ao João Caço, ao João Brito, ao Tiago Dias e à Nicole.

Ao José Dias, um agradecimento especial pelo apoio e carinho diários, pelas palavras doces e pela transmissão de confiança e de força, em todos os momentos.

Agradeço, também aos meus amigos que sempre me apoiaram.

À minha família, em especial aos meus pais, um enorme obrigada por acreditarem sempre em mim, pelo esforço e dedicação que sempre tiveram para que eu pudesse terminar esta etapa e por todos os ensinamentos de vida. À minha tia Dulce e às minhas primas-manas Inês e Violeta pelo apoio e pela forma como me acolheram e integraram em Lisboa.

Por fim, mas não por último, queria agradecer a Deus pela oportunidade e pela maneira como guiou esta tese, que acredito ter sido uma bênção.

Abstract

For bacterial cells to enlarge and divide, peptidoglycan must be cleaved by specific hydrolases so that new subunits can be incorporated into the mature cell wall. The most important murein hydrolase of the opportunistic human pathogen *Staphylococcus aureus* is ATL, a 137.5 kDa bifunctional protein with two domains: AM and GL that are extracellularly processed and bind to the staphylococcal surface at precise locations of the equatorial surface rings. Based on observations that showed that *atl* mutants, constructed in different *S. aureus* genetic backgrounds, are not all impaired in biofilm formation, and that the GL-DNA interaction impacts biofilm formation in a strain specific way, we hypothesized that the physiological roles of ATL may be strain-specific. Different approaches were used to characterize ATL in different *S. aureus* strains: (i) the *atl* gene was sequenced to identify amino acid differences in the protein that could change its activity or undergo different proteolytic cleavage; (ii) the size of the different ATL processed forms and the cell compartment where they accumulate was assessed; (iii) the expression of ATL was analyzed over time by western blotting; (iv) the impact of DNA on GL lytic activity was determined for heat-inactivated cells, cell wall and peptidoglycan, through lytic assays with the GL purified protein.

The results obtained allowed to identify distinct patterns of ATL protein expression and of proteolytic cleavage that may be the basis for the primary phenotypic differences.

Keywords: Autolysin; *Staphylococcus aureus*; lytic activity; ATL; Glucosaminidase; protein expression.

Resumo

Para as células bacterianas crescerem e se dividirem, o peptidoglicano sofre clivagem por hidrolases específicas de modo a que novas subunidades possam ser incorporadas na parede celular. A hidrolase mais importante de *Staphylococcus aureus*, um agente patogénico humano oportunista, é a proteína bifuncional ATL composta por dois domínios, AM e GL, que são processados extracelularmente e se ligam à superfície da bactéria em locais precisos da superfície equatorial. Com base em observações que mostraram que para mutantes de *atl*, construídos em diferentes linhagens de *S. aureus*, a formação de biofilme não é em todos prejudicada, colocou-se a hipótese de que os papéis fisiológicos da ATL podem ser específicos da estirpe. Diferentes abordagens foram usadas para caracterizar a proteína ATL em diferentes estirpes de *S. aureus*: (i) o gene *atl* foi sequenciado com o intuito de encontrar diferenças de aminoácidos na proteína que poderiam alterar a atividade ou sofrer clivagem proteolítica diferente; (ii) analisou-se o tamanho das diferentes formas processadas do ATL, bem como o compartimento da célula em que o mesmo ocorre; (iii) a expressão de ATL foi analisada ao longo do tempo por Western Blot; (iv) determinou-se o impacto do DNA na atividade lítica do GL em células inativadas, na parede celular e no peptidoglicano, através de ensaios de lise com a proteína purificada GL.

Os resultados obtidos permitiram identificar padrões distintos de expressão da proteína de ATL e clivagem proteolítica que pode ser a base para as diferenças fenotípicas primárias.

Palavras-chave: Autolisina; *Staphylococcus aureus*; atividade lítica; ATL; Glucosaminidase; expressão de proteínas.

Table of Contents

List of Figures

List of Tables

Acronymes

ε	Epsilon
AM	Amidase
CA-MRSA	Community-Associated Methicillin Resistant *Staphylococcus aureus*
BCA	Bicinchoninic Acid Assay
DNA	Deoxyribonucleic Acid
EDTA	Ethylenediaminetetraacetic Acid
EMRSA	Epidemic Methicillin Resistant *Staphylococcus aureus*
GL	Glucosaminidase
GlcNAc	N-Acetylglucosamine
h	Hour
HA-MRSA	Hospital-Associated Methicillin Resistant *Staphylococcus aureus*
HCl	Hydrochloric Acid
HSQC	Heteronuclear Single Quantum Coherence
Km	Kanamycin
LA	Lysogeny Broth Agar
LB	Lysogeny Broth
LTA	Lipoteichoic Acid
min	Minutes
MSSA	Methicillin Susceptible *Staphylococcus aureus*
$MgSO_4$	Magnesium Sulfate
MRSA	Methicillin Resistant *Staphylococcus aureus*
MurNAc	N-acetyl-muramic Acid
MW	Molecular Weight
NaCl	Sodium Chloride
NaN_3	Sodium Azide
Na_2HPO_4	Disodium Phosphate
Na_2SO_4	Sodium Sulfate
NH_4Cl	Ammonium chloride

Ni-NTA	Nickel Nitrile-Triacetic Acid
Nm	Nanometer
NMR	Nuclear Magnetic Resonance
OD	Optical Density
O/N	Overnight
PBP	Penicillin-Binding-Protein
PBS	Phosphate Buffered Saline
PCR	Polymerase Chain Reaction
pI	Isoelectric Point
PP	Propeptide
K	Kelvin
KH_2PO_4	Monopotassium Phosphate
kDa	Kilodalton
Rpm	Revolutions per minute
RT	Room Temperature
SCCmec	Staphylococcal cassette chromosome *mec*
SDS	Sodium Dodecyl Sulfate
SDS-PAGE	SDS-Polyacrilamide Gel Electrophoresis
SNP	Single-nucleotide Polymorphism
TA	Teichoic Acids
TCA	Trichloroacetic Acid
TSA	Tryptic Soy Broth Agar
TSB	Tryptic Soy Broth
UV	Ultraviolet
V	Volt
WTA	Wall Teichoic Acids

Chapter I - Introduction

1. *Staphylococcus aureus*

Staphylococcus aureus are Gram-positive cocci with low DNA G+C content that usually occur as grape-like clusters, and form a fairly large yellow colony on rich medium and are often hemolytic on blood agar. *Staphylococci* are facultative anaerobes that grow by aerobic respiration or by fermentation that yields principally lactic acid. These bacteria are catalase-positive (converts hydrogen peroxide to water) and oxidase-negative, and can grow at a temperature range of 15 to 45 degrees and at NaCl concentrations as high as 15 percent. They are coagulase positive, a marker that allows the distinction between *S. aureus* and other *Staphylococcus* (Kloos, 1997).

1.1. Pathogenicity

S. aureus are frequently found as a commensal in the respiratory tract of humans (Kluytmans *et al*, 1997) but can also act as an opportunistic human pathogen. They are the major cause of nosocomial infections worldwide (Pfaller *et al*, 1988).

In colonization, the relationship with the host is benign and asymptomatic, but break of the cutaneous barrier allows the bacteria to internalize and cause diseases such as skin and soft tissue infections (noninvasive infections). As a pathogen, it is considered versatile bacteria, as it can cause a wide spectrum of infections from impetigo and folliculitis to life-threatening invasive infections, such as bacteremia, pneumonia or endocarditis. In addition, intake of toxins from food products colonized by *S. aureus*, can cause acute gastroenteritis (Boucher *et al*, 2010; Lee, 2003; Projan & Novick, 1997).

1.2. Virulence

S. aureus expresses many potential virulence factors including toxins, immune-modulatory factors, and exoenzymes (Watkins *et al,* 2012).

Most of these virulence factors are cell-surface-associated, helping to avoid phagocytosis and consequently allowing the evasion of host defenses. They usually are involved in one of the following processes: i) adherence of *S. aureus* to surfaces, such as adhesins, coagulase, fibrinogen-binding proteins, clumping factor, and biofilm

polysaccharides; ii) escaping of the host immune system, such as enterotoxins, protein A and leukocidins; and iii) damage of the host including hemolysins, phospholipase C and α-toxin. Toxins, proteases and superantigens, prevent the development of a strong antibody response by promoting the bacterial attack of the host, preventing the development of an antibody response, compromising the immune memory (Foster, 2005; Projan *et al*, 1997).

S. aureus is also insensitive to lysozyme (peptidoglycan hydrolase), a bactericidal protein produced by the innate immune system that is present in most human body fluids such as saliva, sweat and tears, and which production is increased during infection (Bera *et al*, 2005; Levy , 2000; Schindler *et al*, 1997).

The fact that *S. aureus* has the ability to easily acquire genetic information also contributes to virulence, mainly through the acquisition of mobile genetic islands that carry virulence determinants.

1.2.1. Multi-drug resistance

S. aureus, the paradigm among the bacteria of this natural phenomenon, has always been a challenge for anti-microbial chemotherapy (Chambers, 2001).

Initially, staphylococci infections were treated with penicillin, a β-lactam antibiotic discovered in 1928 improving the prognosis of patients with staphylococcal infections, decreasing the extremely high mortality rate. β-lactams inhibit the last step of the cell wall peptidoglycan biosynthesis, inactivating the penicillin binding proteins (PBPs) due to the similarity to their substrate – peptidoglycan terminal D-ala-D-ala. The acquisition of a plasmid encoding for a β-lactamase protein (penicillinase) led to penicillin resistance (Abraham and Chain, 1940); this β-lactamase hydrolyzes the β-lactam ring and consequently inactivates the antibiotic (Ghuysen, 1991). In order to overcome the acquired resistance to this natural antibiotic, semi-synthetic compounds (derivatives of penicillin), modified to resist to β-lactamase action, were developed to combat *S. aureus* penicillin resistant infections: methicillin and its derivatives oxacillin, nafcillin, among others (Plata *et al*, 2009; Moellering, 2012).

Methicillin was introduced clinically in 1959, however only two years later, the first strains of methicillin resistant *S. aureus* (MRSA) were identified, carrying the

exogeneous *mecA* gene (Jevons, 1961). The MRSA phenotype is a multifactorial process that occurs by the acquisition of a staphylococcal chromosome cassette (SCC*mec*) and the expression of several housekeeping auxiliary genes. Besides β-lactams antibiotics (penicillins, cephalosporin and carbapenems), MRSA strains also developed resistance to virtually all other classes of antibiotics that were introduced into clinical practice, such as macrolides, chloramphenicol and tetracycline, that target protein synthesis or fluoroquinolones and rifampicin, that target nucleic acid synthesis (Bambeke *et al*, 2003).

The major resistance element of SCC*mec* is the *mecA* gene. This gene codes for an extra PBP, PBP2a (Reynolds & Brown, 1985). PBP2a has a very low affinity to β-lactams, allowing cell wall biosynthesis to proceed in the presence of the antibiotic (Hartman and Tomasz, 1984). The *mecA* gene is not native to *S. aureus* but was acquired from another species, most probably *S. sciuri* (Couto *et al* 1996; Rolo *et al* 2013), by an unknown mechanism. (Beck *et al*, 1986) Although *mecA* is the main genetic determinant for methicillin resistance, recently, a highly divergent *mecA* gene, *mecC*, was identified with relatively low prevalence rates (Shore *et al*, 2011).

The methicillin-resistant phenotype also depends on the expression of more than 32 housekeeping genes - auxiliary factors, frequently associated with the cell wall peptidoglycan biosynthesis and degradation (Roemer *et al*, 2013; Berger-Bächi *et al*, 1992; de Lencastre *et al*, 1999).

1.2.2. MRSA epidemiology

There are several predominant clonal lineages of *S. aureus*; each clonal lineage is defined as a result of its specific genetic background and to the geographic site of its first identification (Johnson *et al*, 2005). Studies based on the genetic analysis of MRSA isolates from different countries revealed that most cases of Hospital-acquired MRSA (HA-MRSA) infections are caused by a small group of epidemic MRSA (EMRSA) clones, which are highly disseminated worldwide (Tomasz & de Lencastre, 1997; Oliveira *et al,* 2002). Each MRSA clonal lineage received a designation and some of the most successful and well disseminated are the Iberian, Brazilian, Hugarian, New York/Japan, Pediatric and epidemic clones: EMRSA-16, EMRSA-15 and Berlin.

In contrast to MRSA infections at hospital settings, in which infected patients have predisposing risk factors such as an immunocompromised immune system, specific MRSA clones emerged in the community, in the mid and late 1990's, in healthy individuals without hospitalization history – the community acquired MRSA (CA-MRSA) (DeLeo *et al*, 2010; David & Daum, 2010). CA-MRSA strains are usually more virulent and more transmissible, however less resistant to antibiotics in comparison with HA-MRSA. Moreover, CA-MRSA strains carry the smaller SCC*mec* elements of types IV and V which were associated with lower fitness costs, thus promoting increased toxin production and thereby increased virulence (Chambers & DeLeo 2009; DeLeo et al. 2010; Otto 2012).

Several CA-MRSA backgrounds emerged and spread differently in separate geographical areas, however, nowadays CA-MRSA are not restricted to a specific geographic region. USA400 clone is present in Asia, Europe and the USA, USA300 in the USA and Europe, the Southwest Pacific clone in Australia, Europe and South America, the ST59-V clone in Asia and the USA, the European clone in Europe, Asia and the Middle East, and ST398 clone, first associated with colonization in pigs in France, is currently disseminated worldwide, not only in animals but also in humans (Mediavilla *et al,* 2012; Monecke *et al*, 2011; Uhlemann *et al,* 2012).

The expanding community reservoir of CA-MRSA has led to the inevitable infiltration of CA-MRSA into hospitals. This phenomenon has become a major public health threat and it is postulated that CA-MRSA will become the dominant MRSA strain in hospitals, with competitive exclusion of the traditional HA-MRSA strain (Seybold *et al*, 2006).

2. Cell Wall

One of the crucial bacterial structures is the cell envelope and its integrity has to be guaranteed.

The Gram-positive cell envelope consists of two functional layers: a cytoplasmic membrane, surrounded by a thick cell wall. The cell wall is a complex and a highly organized structure that allows bacteria to interact with the environment but also protects them against hostile insults. The Gram-positive cell wall is composed by

diverse structures, being the peptidoglycan their major component (up to 50%) and the teichoic acids (TAs) the key multi-functional components of the cell wall. Many Gram-positive bacteria, such as *S. aureus*, contain two types of TAs; wall teichoic acids (WTA), which are covalently linked to the peptidoglycan layer and lipoteichoic acids (LTA), which are embedded in the membrane via a lipid anchor (Reichmann & Grundling, 2011; Xia *et al* 2010). Besides peptidoglycan and teichoic acids, the cell wall harbors a variety of different polysaccharides, polymers and proteins, like the PBPs.

2.1. Peptidoglycan Biosynthesis

Peptidoglycan, also called murein, is a polymer that consists of long glycan chains of alternated disaccharide units (*N*-acetyl-glucosamine and *N*-acetyl-muramic acid) that are cross-linked via flexible peptide bridges to form a strong but elastic structure that protects from lysis due to the high internal osmotic pressure (Ehlert & Holtje, 1996; Holtje, 1998; Nanninga, 1998; Schleifer & Kandler, 1972) (Figure 1).

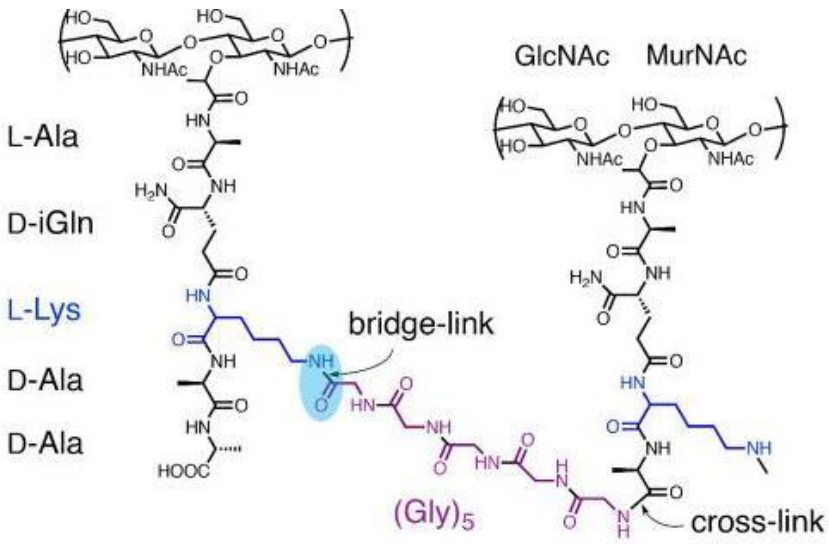

Figure 1 - Chemical structure of *S. aureus* peptidoglycan: disaccharide units cross-linked through an inter-peptide bridge consisting of five glycines to connect the ε-amino group of L-Lys in the third position of one stem (bridge-link, highlighted) to the D-Ala in the fourth position of the connected stem (cross-link) with the concomitant cleavage of the terminal D-Ala. (Zhou & Cegelski, 2012)

Peptidoglycan and its biosynthetic pathway is the target of several antibiotic classes including β-lactams and glycopeptides (Plata *et al*. 2009).

In *S. aureus*, peptidoglycan synthesis begins in the cytoplasm where the precursor UDP-MurNAc-pentapeptide is assembled. It consists of a unit of N-acetyl-muramic acid (MurNAc) that is attached to a pentapetide chain L-alanine-D-glutamate-L-lysine-D-alanyl-D-alanine (Vollmer *et al*, 2008). Then, UDP-MurNAc-pentapeptide is transferred to a membrane-bound lipid carrier by the action of MraY, forming lipid I. UDP-GlcNAc is added to lipid I by the action of MurG, leading to the formation of lipid II (van Heijenoort, 2007), that is transported through the membrane by the action of FtsW flippase and is polymerized through transglycosylation (to extend the glycan chains) and transpeptidation (crosslinking between stem peptides of different glycan strands). In *S. aureus* most of the pentapeptide chains of adjacent macromolecules are linked by pentaglycine interbridges between the penultimate D-alanine of one peptide chain and the free amino group of the lysine of the other chain. This is achieved through the transpeptidation activity of the so-called penicillin-binding proteins (PBP's), which also catalyze the transglycosylation reaction. (Goffin *et al*, 1998) The peptidyltransferases (FemX, FemA and FemB) are responsible for the addition of the five glycine residues of the bridge, in a reaction catalyzed at the membrane level. (Figure 2)

Additional modifications to the peptidoglycan structure occur in many bacterial species including modifications to the glycan chains, modifications to the stem peptide, such as the amidation of the glutamate residue by the proteins MurT and GatD, and incorporation of cell wall polymers (Figueiredo *et al*, 2012).

The thickness of the murein layer, in *S. aureus,* varies between 20 to 400 nm (50% of the cell wall). It is a dynamic macro-molecule that suffers permanent biosynthesis, maturation, recycling, assembly and disassembly in order to maintain the cell shape, and allow for cellular growth and division. (Figure 2)

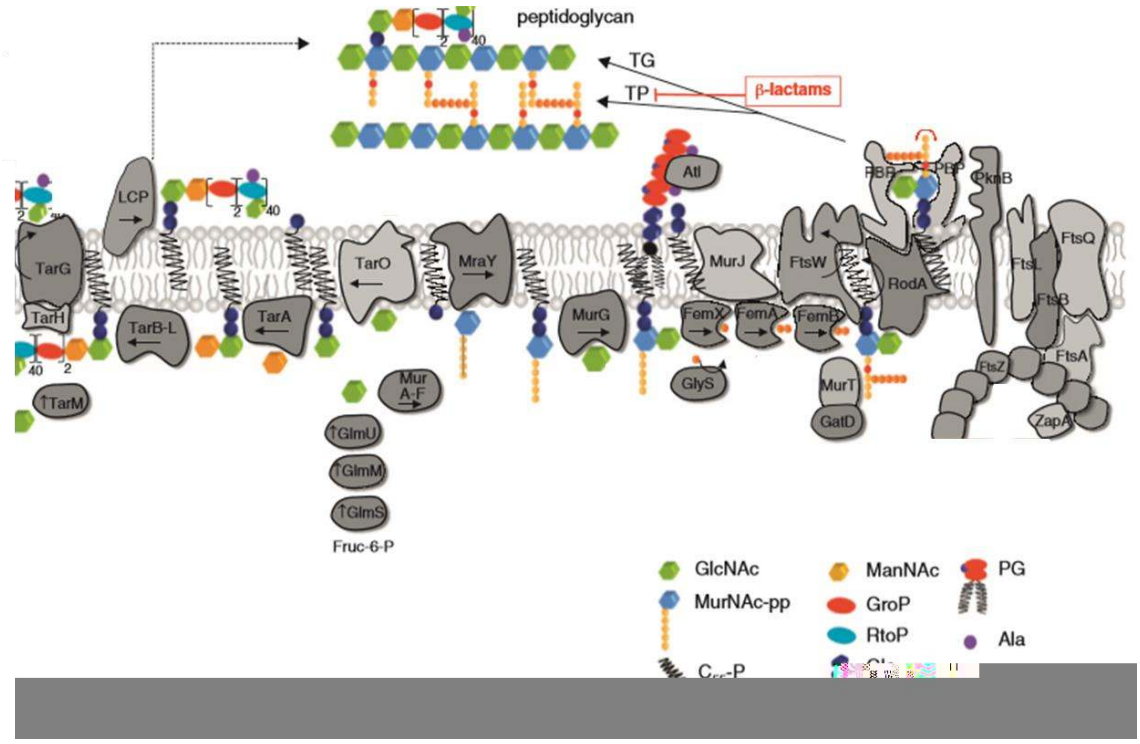

Figure 2 – **Schematic representation of coordinated cell wall biosynthesis and cell division in *S. aureus*** (adapted from Roemer *et al,* 2013).

2.2. Hydrolases

Synthesized peptidoglycan units are incorporated into the intact cell wall layer after cleavage by peptidoglycan hydrolases. A proper balance between peptidoglycan synthesis and degradation during bacterial growth is essential. In general, peptidoglycan hydrolases are thought to play an important role in cell wall turnover, cell division, and cell separation, and in the lysis of bacteria induced by the β-lactam antibiotics (Biswas *et al,* 2006).

S. aureus produces several peptidoglycan hydrolases, such as N-acetylglucosaminidases, N-acetylmuramidases, N-acetylmuramyl-L-alanine amidases, lytic transglycosylases and endopeptidases. Only the genes *atl*, *sleI* and *lytM* and their products have been characterized (Figure 3).

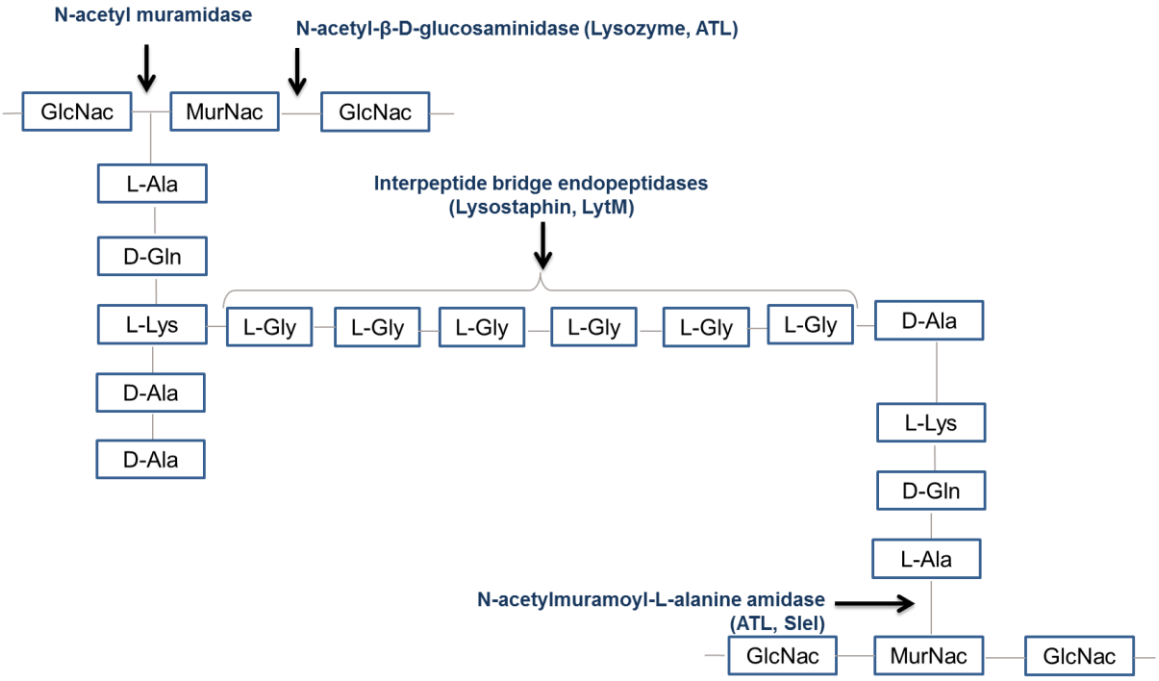

Figure 3 – Murein hydrolases targets within *S. aureus* peptidoglycan. The arrows indicate the cleavage sites (adapted from Szweda *et al*, 2012).

SleI is a 32kDa protein with N-acetylmuramyl-L-alanine activity and is involved in cell separation after division in *S. aureus* (Heilmann *et al*, 2005). LytM is a 32 kDa protein with glycylglycine endopeptidase activity, being able to hydrolyse the glycyl-glycine bonds of *S. aureus* cross bridges. Ramadurai (1997 and 1999) reported that LytM plays a role in cell growth as it is distributed on the cell surface uniformly. Other peptidoglycan hydrolases with N-acetylmuramyl-L-alanine amidases activity were described in *S. aureus*, including LytA (23 kDa), LytH (33kDa) and LytN (46kDa).

2.3. ATL – The major autolysin of *Staphylococcus aureus*

The most prominent murein hydrolase of *S. aureus* is ATL, a 137.5 kDa bifunctional protein (Oshida, 1995). ATL protein consists of a signal peptide, a pro-peptide, a catalytic domain with N-acetylmuramyl-L-alanine amidase activity (AM), three repeats (R1-R3), and a C-terminal catalytic domain with N-acetylglucosaminidase activity (GL). After secretion, the precursor protein is processed extracellularly to yield the mature amidase (AM) and glucosaminidase (GL) proteins. (Figure 4)

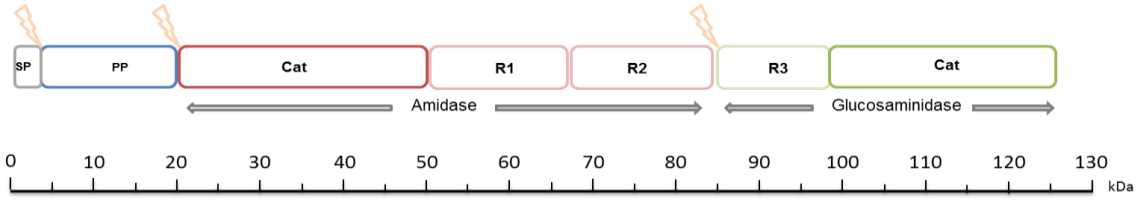

Figure 4 – Domain arrangement of the bifunctional ATL precursor protein. Arrows (lightning) indicate the post-translational cleavage sites. SP- signalpeptide; PP- propeptide; cat- catalytic domains; R1 R2 R3- repeat domains.

The amidase (63.3 kDa) cleaves the amide bond between the N-acetyl muramic acid in the glycan backbone and L-alanine in the stem peptide, contains an enzymatic domain and two repeat domains involved in localization and substrate recognition (R1 and R2, that can each be further divided into an a-type and a b-type subunit) (Biswas, 2006; Marino *et al*, 2002). The amidase repeats R1R2 are responsible for attaching the enzyme to the cell wall and do not contribute to lytic activity (Oshida, 1995; Biswas, 2006). The structure of AM from *Staphylococcus epidermidis* is already determined (Figure 5). This domain, without repeats, adopts a globular, mixed α/β fold, with six stranded, central β-sheet surrounded by seven α-helices (Zoll *et al*, 2010). In the center of the recessed area is a zinc ion. R2ab resembles a half-open β-barrel formed by a semi-circular, four stranded β-sheet, and the two subunits are arranged in a similar orientation.

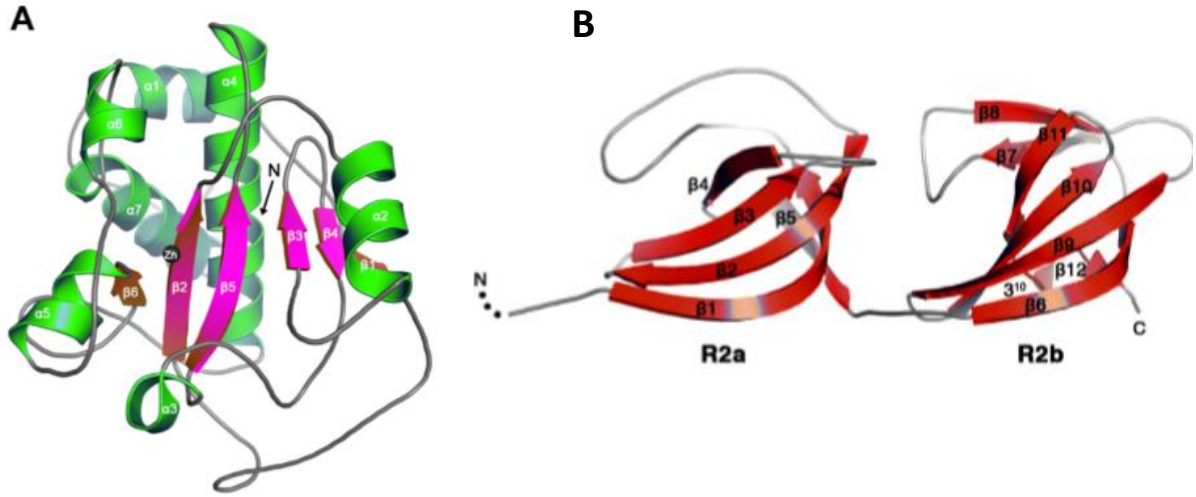

Figure 5 – (A) **Structure of the catalytic domain of AmiE amidase (without repeats R1,2) of *S. epidermidis* AtlE**. Helices and strands are shown in green and pink respectively. (B) **Structure of the Atl repeats R2ab**. R2a and R2b have a similar β-structure that is connected with a flexible linker with R1a. (Götz *et al,* 2013)

GL (53.6 kDa) hydrolyzes the bond between N-acetyl-β-D-glucosamine and N-acetyl muramic acid and contains an enzymatic domain and a single repeat domain (R3) (Oshida, 1995). The structure of GL domain has not been elucidated yet.

The differences in structure of the repeat domains of these two enzymes might reflect the differences of the recognition sites on staphylococcal cell walls. The *atl* gene was probably developed through fusion of AM and GL genes (Oshida, 1995).

2.3.1. Role of ATL in Cell Division

S. aureus is known to occur singly, in pairs, in short chains, and in irregular clusters (Bergey's Manual, 8th ed.), dividing in an unusual way, as it switches division plane in three consecutive perpendicular orientations in successive division cycles (Tzagoloff & Novick, 1977). *S. aureus* cells divide by forming a septum which is split, becoming the new hemisphere of each daughter cell (Giesbrecht *et al*, 1976; Amako & Umeda, 1997).

The binding of both AM and GL to the staphylococcal surface occurs at precise locations of the equatorial surface rings, not only at the septum of dividing cells but also at a perpendicular surface ring that marks the future cell division site (Sugai *et al*, 1997; Baba and Schneewind, 1998).

The mechanism by which ATL-hydrolase is targeted to the equatorial surface ring is based on an avoidance strategy by WTAs, which prevents binding of ATL. As WTAs are abundant in the cell wall but not at the cross-wall region, ATL is able to bind to this region. There are at least two possible mechanisms for the specific localization of ATL at the septal sites of the cell surface. One is that ATL protein is synthesized, translocated at the cell division site, and localized with an anchoring component. The other is that ATL is secreted into the culture medium and reabsorbed to an anchoring component via ligand-receptor interaction (Schlag *et al*, 2010; Yamada *et al*, 1995). (Figure 6)

The ring structure of the localization of the *atl* gene products raises many interesting questions such as the identification of the components of the cell wall that interact with ATL domains and also the regulation of ATL different enzymatic activities.

Deletion mutants of *atl* form large cell clusters in which the walls of individual cells appear to be interlinked with other cells, indicating a severe defect in cell separation (Biswas *et al,* 2006).

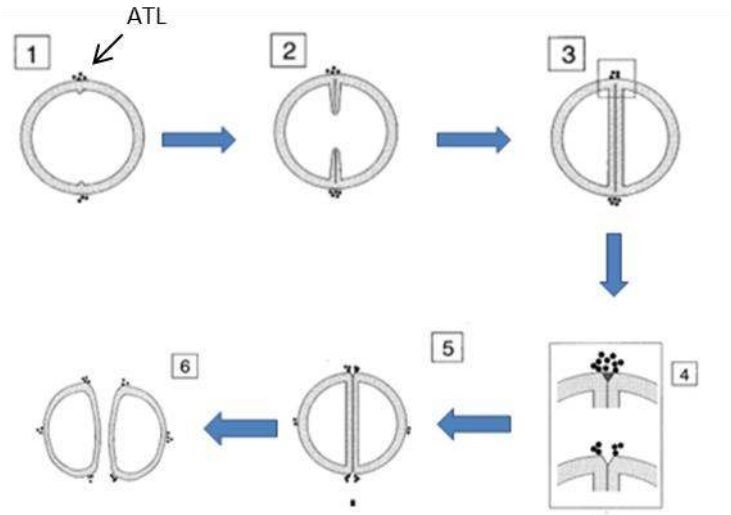

Figure 6 - **Model for the function of *atl* gene products in cell-cell separation**. Localization of *atl* gene products at the cell surface for the different cell division phases; 1 – beginning of septum formation; 2 – septum invagination; 3 – complete septum formation; 4 – detail of murein hydrolysis at the septum limits; 5 - ATL localizes at the future cell division site; 6- cell division (adapted from Yamada *et al*, 1995).

2.3.2. Role of ATL in Biofilm formation

Colonization of human nares, among other surfaces, with *S. aureus* usually involves the establishment of biofilms (Iwase *et al*, 2010). These aggregates occur in natural and industrial environments, but also in hospital settings. Biofilm formation begins with the initial adhesion of bacteria to the host epithelial surfaces; subsequent release of bacterial polysaccharides, proteins and DNA leads to the formation of an extracellular matrix that involves the biofilm community. After biofilm growth and maturation, shedding and release of bacterial cells, promotes invasive disease and dissemination into host tissues (Sadykov, 2012; Archer, 2011). Cell death and lysis is a necessary and, apparently, controlled process during the development of *S. aureus* biofilm (Rice *et al,* 2007).

A link between ATL hydrolase and the formation of biofilm has been recurrently reported. The disruption of the *atl* gene caused a dramatic decrease in the ability to form

biofilm (Bose *et al*, 2012; Houston *et al*, 2011; Boles *et al*, 2010; Heilman *et al,* 1996) and the adhesion characteristics of the deletion mutants resembled those of DNase I-treated samples (Das *et al,* 2010). The currently accepted model for the role of ATL in biofilm formation defends that this protein is directly involved in cellular autolysis and genomic DNA (an important building block of the biofilm matrix) release (Boles *et al,* 2010). *S. aureus* biofilms may include bacterial DNA as part of the extracellular matrix (Kaplan *et al*, 2012; Mann *et al*, 2009) which its released through the activity of ATL (Houston *et al*, 2011; Rice *et al,* 2007). On the other hand, ATL directly contributes to the attachment of cells to the surface during the early stages of biofilm formation (Houston *et al*, 2011). The repeat domains of ATL have been shown to bind various host extracellular matrix proteins, including vitronectin and fibronectin (Heilmann *et al,* 2005; Heilmann *et al,* 1997; Hell *et al*, 1998).

The recently reported DNA-binding capacity of the catalytic GL domain of ATL may confer another function for this hydrolase in biofilm development: GL could provide an attachment point between the cell surface and the biofilm matrix (Grilo *et al*, 2014).

2.3.3. ATL-DNA association

Recently, Grilo *et al* (2014) reported that ATL is able to bind DNA molecules, suggesting multiple possible roles for such activity. This DNA-binding activity is not sequence specific and does not require interaction with other proteins. It is present in the unprocessed ATL protein, in the catalytic region of the GL domain and in the repeat domains as well. The GL catalytic domain showed DNA-binding activity independent of the presence of the R3 repeat unit, and DNA-binding activity of the AM domain is, in contrast to the GL domain, restricted to the repeat regions. It is speculated that this binding capacity is primarily related to the capture and/or anchoring of extracellular DNA molecules.

3. Thesis objectives

Preliminary observations (Grilo *et al,* unpublished) showed that *atl* mutants, constructed in different *S. aureus* genetic backgrounds, are not all impaired in biofilm formation. Also, a role for GL-DNA binding capacity in biofilm formation was observed for some strains, while not for others (see results in annex 1).

Facing these observations, we hypothesized that the physiological roles of ATL protein are strain-specific.

The main objective of this thesis is to characterize ATL protein regarding strain specificity:

1- The different processed forms and the cell compartment where the cleavage occurs, in different *S. aureus* backgrounds (MRSA and MSSA strains).
2- Analyze the expression of ATL along time in the different strains.
3- Analyze the impact of DNA on GL lytic activity on the peptidoglycan of several *S. aureus* lineages.
4- Characterize GL-DNA interaction by NMR.

Chapter II - Materials and Methods

1. Strains

In this study, *S. aureus* strains COL, NCTC 8325, WIS, HDE 288, MW2, UAMS-1 and JE2 were grown at 37ºC with aeration in Tryptic Soy Broth or Agar (TSB/TSA) (Difco Laboratories, USA), and *Escherichia coli* strains were grown at 37ºC in Lysogeny Broth or agar (LB/LA) (Difco Laboratories). These strains and their genotype are listed in Table 1.

Table 1 – Strains and plasmids used in this study.

Strain or plasmid	Genotype or Description	Source or reference
Strains		
Staphylococcus aureus		
COL	HA-MRSA; archaic clone, SCC*mec* type I Tet^r, Strep^r	Rockefeller University Collection
NCTC 8325	MSSA	Novick, 1991
WIS	Taiwan clone, SCC*mec* type V CA-MRSA	O'brien *et al*, 1999
HDE 288	HA-MRSA; Pediatric clone, SCC*mec* type VI AMS^r, Cft^r, Oxa^r, Pen^r	Sá-Leão *et al,* 1999
JE2	CA-MRSA; USA 300 clone	Diep *et al*, 2006
MW2	CA-MRSA; USA400 clone, SCC*mec* type IV	CDC, 1999
UAMS-1	MSSA	Gillaspy *et al*, 1995
Escherichia coli		
BL21(DE3)	F–ompT gal dcm lon hsdSB(rBmB) k(DE3 [lacI lacUV5-T7 gene 1 ind1 sam7 nin5])	Invitrogen
Plasmids		
pET28a(+)	*E. coli* expression vector	Novagen
pET-GL	pET28a(+) expressing GL as a N-terminal His-tag fusion (fragment amplified with Pexp3 and Pexp4)	Grilo *et al,* 2014
pET-AM	pET28a(+) expressing AM as a N-terminal His-tag fusion (fragment amplified with Pexp1 and Pexp5)	Grilo *et al,* 2014

2. DNA Methods

Chromosomal DNA from strains was extracted using Wizard Genomic DNA Purification kit (Promega, USA) as suggested by the manufacturer, with some modifications, namely, an initial cell lysis step, performed in Tris pH8 supplemented with 10 mg/ml of lysostaphin (AMBI PRODUCTS LLC, USA) and 30 µg/ml of RNase (SIGMA, USA).

2.1. PCR and sequencing

Routine PCR (polymerase chain reaction) amplification was performed with NZYTaq DNA polymerase (Nzytech, Portugal). The primers used are listed in Table 2. PCR products were purified with DNA Clean & Concentrator^{TM}-5 (Zymo Research, USA).

Table 2 – Primers used for PCR amplification.

Primer	Sequence	nt
PAM fw BamHI	CCAGGATCCGCTTCAGCACAACCAAGATCAG	31
pGL rv XhoI	CCACTCGAGTTTATATTGTGGGATGTCG	28
PreAM fw	ATGAATGCCCAATGTCATGC	20
AM rv	AGTAGTTACTTTAGGTGTCGC	21
PcompATL fw SalI	CGAGTCGACGATTTGTCACGTCACC	25
PAMR2 rv SalI	CCAGTCGACTTAGGTAGTTGTAGATTGCG	29
PR1R2R3GL fw NcoI	GCTCCATGGCTCCTACTACACCATCAAAACC	31
PAM rv SalI	CCAGTCGACTTATTTTACAGCTGTTTTTGG	30
PR2R3GL fw NcoI	GCACCATGGCTCCTACACCAACACCTAAGCC	31
pGLSH3 rv SalI	CCTGTCGACTTAATGCTTAACATCATTAAAGTTAGC	36
PGL fw BamHI	CGTGGATCCGCTTATACTGTTACTAAACC	29
PGL rv SalI	CCAGTCGACTTATTTATATTGTGGGATGTCG	31
PGLSH3fw	GATGTTAAGCATGCAATGGATACG	24
PosGL rv	ACGTTGCGAATTGATTGAAGC	21

PCR products were sequenced at STAB VIDA (Portugal), and the sequence traces were analyzed using the software DNAstar Lasergene SeqMan Pro (Version: 7.1.0).

3. Fractionation of culture contents

Culture samples were taken over time corresponding to the following OD_{620nm}: 0.1, 0.2, 0.4, 0.6, 1, 2, 3, 4, 6 and at late stationary phase (≈24h). Cells were harvested by centrifugation (10 000g, for 10 minutes at 4ºC) and the supernatant and the pellet were separately stored at -20ºC and later processed as follows.

Supernatant

The supernatant protein precipitation was performed using 1/10 volume of TCA, during 17h, at -20ºC. The protein fraction was collected by centrifugation at 13 000 rpm 4ºC, 10 minutes (SIGMA 3-16K, 12155 rotor, Sartorius, Germany). The protein pellet was rinsed with ice-cold acetone and centrifuged at 13 000 rpm 4ºC for 10 minutes. The supernatant was discarded and the dried pellet ressuspended in 500µl PBS 1x.

Pellet

In order to obtain the same cell number, different volumes of culture were used, as showed in Table 3. The pellet was washed in 1ml of ice-cold 50mM Tris-HCl (pH7.5)-150mM NaCl and centrifuged at 10 000 rpm, 4ºC for 10 minutes. Then, the membrane-associated proteins were extracted by ressupending the pellet in 100µl of 4% SDS and incubating at room temperature (RT) for 30 minutes with stirring. The SDS suspensions were centrifuged at 13 000 rpm (Biofuge Pico Heraeus), for 15 minutes at RT. The supernatants were stored in aliquots at -20ºC.

Table 3 – Culture volumes taken at different $OD's_{620nm.}$

OD_{620nm}	Volume (mL)
0.1	50
0.2	25
0.4	12.5
0.6	8.3
1	5
2	2.5
3	1.7
4	1.25
6	0.83

3.1. Protein analysis by SDS-PAGE and Western Blot

To verify the integrity of the protein extracts, protein samples were analyzed under denaturing conditions using SDS-polyacrylamide gel electrophoresis (PAGE), with the mini-PROTEAN system (BIO-RAD, USA). Before electrophoresis, the samples were mixed in a ratio of 1:2 with 19:1 (Laemmli: β-mercaptoethanol) solution, incubated at 95ºC for 5 min and then 10 min on ice. Electrophoresis was performed in running buffer (24 mM Tris-base, 191 mM Glycine, 3.46 mM SDS) at 30 mA for 1-1.5 h. Samples were analyzed in 10% SDS-PAGE along with molecular weight marker (ColorBurst Electrophoresis Marker, Sigma or Precision Plus Protein™ All Blue Standards, BIO-RAD).

Proteins were transferred to a nitrocellulose membrane (Amersham Hybond ECL Nitrocellulose, 0.45 μm from GE Healthcare, UK) using the Mini Trans-blot electrophoretic transfer cell (BIO-RAD) and transfer solution (25 mM Tris-base, 192 mM Glycine, 10% Ethanol). Blotting was performed at 4ºC for 90 min at 100 V with agitation. After blotting, the membrane was incubated overnight in blocking solution (PBS-Tween and 5% w/v low-fat milk), washed with PBS-Tween and probed with the primary antibody anti-GL or anti-AM (Grilo et al, unpublished), in a ratio of 1:1500 for 2 h and 1:1000 for 5h, respectively. The membrane was then washed, immersed in fresh blocking buffer and incubated with secondary antibody (anti-rabbit IgG) (Perkin Elmer, USA) in a ratio of 1:20000 for 30min. After a final washing step, the membrane was incubated with chemiluminescence detection solution for 1 min (Western Lightning Plus-ECL, PerkinElmer, USA) and exposed to autoradiographic film (Amersham HyperfilmTM ECL GE Healthcare) for appropriate periods of time. The film was processed manually by immersion in developing and fixing reagents.

4. GL-mediated Lysis Assays

Three different substrates were used to analyze the lytic activity of GL: (i) heat-inactivated cells, (ii) cell wall, and (iii) peptidoglycan. Samples were prepared as described in the next sections (4.1 – 4.3). Heat-inactivated cells were diluted to an $OD_{600\approx}$ 0.4 in Tris pH7.5. Cell wall and purified peptidoglycan were prepared Tris pH7.5 to an initial concentration of 4mg/mL. Low-molecular weight salmon sperm DNA (Sigma) (0.5 and 0.05 mg/mL) and purified protein ATL-C (GL domain without

the repeat region, Grilo *et al*, 2014) (5ng/µl) were added to the wells, as needed. Mutanolysin (5µg/mL) and lysostaphin (5µg/mL) were used as positive controls for lytic activity.

Lysis assays were performed in sterile nontreated 96-well microplates (Brandplates®, Brand, Portugal) at 37ºC with shaking for 10h, taking readings (600nm) with 10 minutes interval in a microplate reader Sprectra Max190 (Molecular devices, USA).

4.1. Purification of heat-inactivated cells

S. aureus strains were grown at 37°C with stirring to an OD of ≈0,3 and cells were harvest by centrifugation at 10 000 rpms at 4ºC for 10 minutes (Sorvall RC-5C 19 Plus, SLA-150 rotor, Kendro Laboratory Products Newtown, USA). The pellets were ressuspended in cold water and cells were boiled in SDS (to a final 4% SDS concentration) for 30 minutes. The cultures were kept at RT O/N. The SDS was removed by washing the cells with hot water until no SDS is detected in the ressuspended pellet through the Hayashi method. The pellet cells were kept in H_2O with 0,05% NaN_3.

4.2. Cell wall extraction

To extract the cell walls, the procedure of section 4.1. was performed and subsequently the cells were broken by glass beads (Glass beads, acid-washed, 425-600 µm, Sigma) using the Fastprep apparatus (Fastprep FP120, Bio 101 Savant, France), 3 times, 40 seconds at speed 6. The samples were cooled on ice between runs. Glass beads were removed by filtration using a vaccum filter (porosity 3). The filtrate was centrifuge in corex tubes for 5 minutes at 2 000 rpm, RT, to remove unbroken cells and large cellular debris. The supernatant was centrifuged for 15minutes at 15 000 rpm, RT. Pellets were ressuspended in 100mM Tris (pH 7.5).

To purify the cell walls, the samples were incubated with $MgSO_4$ (20 mM), DNAse and RNAse (10 and 50 µg/ml, respectively) at 37ºC for 2h. Afterwards, $CaCl_2$ (10 mM) and trypsin (100µg/ml) were added and the samples were incubation proceeded O/N with agitation. To inactivate the enzymes, SDS was added to a final concentration of 1% and the samples boiled for 15minutes.

SDS was removed by 2 washes with H_2O, centrifuging at 15 000rpm for 15 minutes. The pellet was incubated in 8M $LiCl_2$, for 30 minutes at 37ºC and centrifuged for 15 minutes at 15 000 rpm at RT. The pellet was incubated in 0.1M EDTA (pH 7.0), for 30 minutes at 37ºC and again centrifuged. After 4 washings with H_2O the pellet was lyophilized O/N in Speedvac (Savant™ Speedvac™ Concentrator, USA).

4.3. Purification of Peptidoglycan

Peptidoglycan purification was performed following the procedures of sections 4.1. and 4.2.. The lyophilized pellet (section 4.2) was treated with 48% hydrofluoric acid, for 48h at 4ºC with agitation. After incubation, H_2O was added and a pellet was obtained by centrifugation (45min at 20 000 rpm, 4ºC). This step was repeated. The pellet was ressuspended in 10mM Tris (pH 7.0), followed by centrifugation. Three H_2O washing steps were performed. The pellet was lyophilized O/N in Speedvac.

5. Protein expression and purification

ATL-C protein (GL domain without the repeat region) (Grilo *et al*, 2014) was expressed using two different procedures, according to the final objective: i) protein for the lysis assays, and ii) protein for the NMR assays.

5.1. Expression of ATL-C protein in complex medium for digestion assays

ATL-C protein was expressed in *E. coli* BL21(DE3)+PET28a-ATL-C. Cells transformed with the appropriate recombinant plasmid were grown in LA medium supplemented with Kanamycin (30 µg/ml of Km) at 37ºC.

A colony was inoculated in 500mL of auto-induction medium (LB medium supplemented with 2mM $MgSO_4$, 10mL 50x5052 (0.5% glycerol, 0.05% glucose and 0.2% lactose), 25mL 20xNPS (see annex 3) and Kanamycin 30µg/ml), grown at 37ºC for 17h and cells were harvested (12000 rpm for 10 min) (Sorvall RC-5C 19 Plus) and ressuspended in 20mL lysis buffer (50mM Na_2HPO_4; 300mM NaCl; 10mM Imidazole; pH8) and 10 UmL^{-1} benzonase (Novagen, Germany) (4µL).

After cell disruption performed with a French Press (FA-032 (40k) standard cell at 12000 psi from Thermo Electron Corporation), and removal of cellular debris

and membranes by centrifugation (12000 rpm for 1 h), the lysate was subsequently purified as described in the next section.

5.1.1. Manual protein purification using Ni-NTA matrix

The column was charged with Ni-NTA agarose (Qiagen, USA) and equilibrated with 20mL of water and 20mL of lysis buffer. The lysate was loaded onto the column and an aliquot was collected (flow-through). 20mL of wash buffer (50mM Na_2HPO_4; 300mM NaCl; 30mM Imidazole; pH8) was used for the washing steps and 2mL of Elution Buffer (50mM Na_2HPO_4; 300mM NaCl; 250mM Imidazole; pH8) for collecting 5 elutions. Finally, the column was washed with water and 30% ethanol and stored at 4ºC. Aliquots were collected at each step.

To verify the protein purity level, the protein samples were analyzed under denaturing conditions using SDS-polyacrylamide gel electrophoresis (PAGE), as described before, in section 3.1.

5.2. Expression of ATL-C protein in Minimal Medium for NMR analysis

ATL-C protein was expressed in *E. coli* BL21(DE3)+PET28a-ATL-C. To test the expression conditions, the assays were performed in small-scale, using 200 ml of bacterial culture, while, to obtain high quantities of protein, expression was performed in large-scale, using 500mL to 1L of bacterial culture. The method of cell disruption adopted was mechanical disruption with French Press as before.

Small-scale:

A colony was inoculated in 10mL of non-induction minimal medium (50mM Na_2HPO_4, 50mM KH_2PO_4, 5mM Na_2SO_4, 50mM NH_4Cl, 2mM $MgSO_4$, 0.2x trace metals (see annex 3), 0.5% glucose) and grown at 37ºC for 7h. Subsequently, 2% of the volume was inoculated in 25 mL of fresh non-induction minimal medium and the culture was grown at 37ºC for 17h. Then, 2% of the culture was transferred to 200mL of induction minimal medium (50mM Na_2HPO_4, 50mM KH_2PO_4, 5mM $NaSO_4$, 50mM NH_4Cl, 2mM $MgSO_4$, 0.2x trace metals, 200µL 50x5052). After 24 h of incubation at 37ºC, cells were harvested (12000 rpm for 10 min) (Sorvall RC-5C 19 Plus) and ressuspended in 20mL lysis buffer and 10 UmL^{-1} benzonase (adapted from Studier, 2005).

After cell disruption performed using a French Press and removal of cellular debris and membranes by centrifugation, the lysate was subsequently purified as described in 5.1.1 section and analyzed by SDS-PAGE as described in section 5.1.2..

Large-scale:

The procedure was the same as for small-scale, with the corresponding volumes scalled-up for 1L of bacterial culture.

5.2.1. Expression of ATL-C protein in Minimal Medium for ^{15}N NMR analysis

The protein expression procedure was performed as optimized for minimal medium (section 5.2), with the exception that instead of 50mM NH_4Cl, labeled $^{15}NH_4Cl$ (Sigma) was added to the same concentration, with the corresponding volumes scalled-up for 500mL of bacterial culture.

5.3. Desalting and protein concentration

Desalting and buffer exchange were performed using PD-10 desalting columns (GE Healthcare) to 100mM Tris (pH7.5). PD-10 Desalting Columns contain Sephadex G-25 Medium, which allows separation of high molecular weight substances from low molecular weight substances; small molecules like salt and other impurities are efficiently separated from the high molecular weight substances of interest.

The samples were concentrated using Amicon® Ultra-4 (10 k) Centrifugal Filter Units (Merck Millipore, USA). This device provides efficient concentration and desalting of macromolecules by ultrafiltration using Millipore's Ultracel® YM regenerated cellulose anisotropic membranes. Centrifugal force drives solvents and low molecular weight solutes through the membrane while the macromolecules remain inside the sample reservoir.

5.4. Protein quantification

The total amount of protein present in each fraction collected was estimated by UV absorption at 280 nm (NanoDrop ND-1000, Fisher Scientific, Spain), using extinction coefficient and protein molecular weight calculated with the online tools

ProtParam and Compute pI/MW (ExPASy, Bioinformatics Resource Portal) specific for the target protein (ATL-C: ε= 64860 cm^{-1}/M; MW = 39639.6641 Da).

Protein concentration from the extracts (section 3) was measured with BCA assay (Pierce) in a microplate reader.

6. NMR analysis

NMR experiments were performed at 298 K in a Avance II+ 600-MHz spectrometer (Bruker, Germany) equipped with 5-mm TCI cryoprobe. Proton chemical shifts were referenced against external DSS while nitrogen chemical shifts were referenced indirectly to DSS using the absolute frequency ratio. Data was processed using the Topspin 3.1 package (Bruker).

A 1 mM solution of ^{15}N-labeled ATL-C in 25mM Tris-DCl buffer (10% $2H_2O$, pH=7.5) 75mM NaCl, was titrated.

Chapter III – Results

Preliminary results (see annex1) suggest that the physiological roles of ATL autolysin and in particular, its association with DNA (Grilo *et al*, 2014) is dependent on the genetic background of *S. aureus.* Thus, with the purpose of characterize the *S. aureus* ATL protein, regarding strain specificity, different approaches were designed and different genetic backgrounds were used, namely strains COL (HA-MRSA, archaic clone), WIS (CA-MRSA, Taiwan clone), HDE288 (HA-MRSA, pediatric clone), UAMS-1 (MSSA, , JE2 (CA-MRSA, USA300), NCTC8325 (MSSA, laboratory strain) and MW2 (CA-MRSA, USA400).

1. Determination of *atl* gene SNPs

In order to compare the nucleotide sequence of *atl* gene of the different strains, the *atl* gene was fully sequenced for strains for which the genome sequence was still undetermined, namely WIS, HDE288 and JE2.

The sequence length of *atl* gene, including the promoter region, is approximately 4000 bps; amplification of this region was performed in 6 separate DNA fragments (fragments A to F), as shown on Table 4 and Figure 7.

Table 4 – *atl* gene fragments amplified and primers used for PCR amplification.

DNA fragment	Primers	Length (bps)
A	PcompATLfwSalI + PAMR2rvSalI	1431
B	PR1R2R3GLfwNcoI + PAMrvSalI	1053
C	PR2R3GLfwNcoI + pGLSH3rvSalI	1392
D	PGLfwBamHI + PGLrvSalI	1446
E	PreAM fw + AM rv	941
F	PGLSH3fw + PosGL rv	915

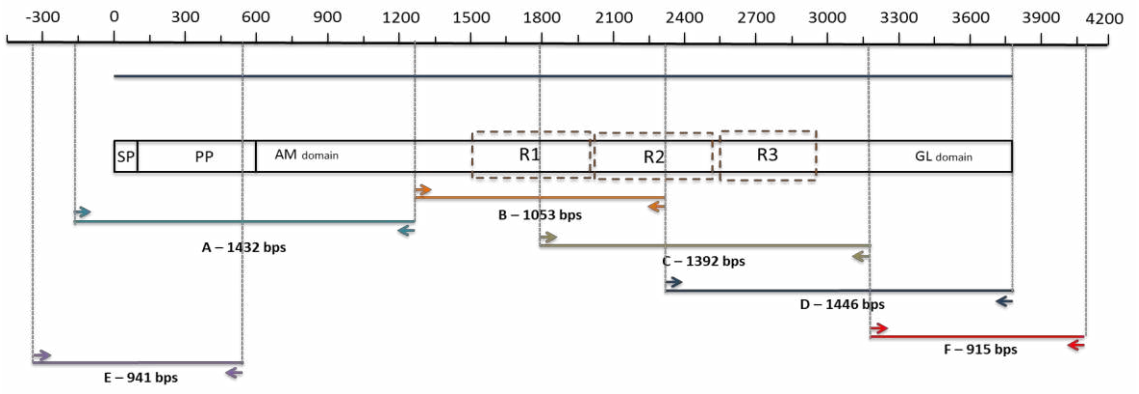

Figure 7 – *atl* PCR reactions scheme. The *atl* sequence, including the promoter was approximately 4500 bps. Six fragments of approximately 1000 pbs, designated A to F, were amplified and sequenced.

The PCR products were sequenced separately and the resultant full sequences were assembled and aligned, using DNASTAR Lasergene software, with the sequences already available in the databases for strains, COL (CP000046), UAMS-1 (JTJK00000000), NCTC8325 (NC_007795) and MW2 (BA000033). Strain COL was used as reference. A high number of nucleotide differences and high diversity (nucleotide differences specific to one strain) was observed among the *atl* coding sequences of the different genetic backgrounds (Table 5). The three strains that showed higher nucleotide diversity were UAMS-1 (>100 nucleotide substitutions, 1 insertion and 3 deletion events), HDE288 (27 nucleotide substitutions and 1 deletion event) and JE2 (37 nucleotide substitutions and 1 insertion event). The two possible candidate promotor regions (Oshida *et al*, 1994) were identified upstream from the start codon and no nucleotide substitution was observed (Figure 8).

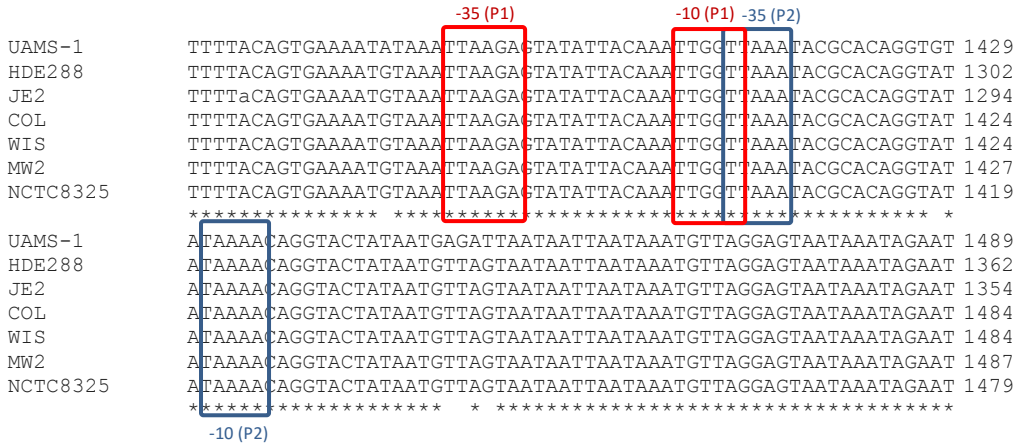

Figure 8 - Alignment of the two promoter candidates sequences of ATL of *S. aureus* strains UAMS-1, HDE288, COL, WIS, MW2, NCTC8325 and JE2 (CLUSTAL Omega). In red are highlighted the Promotor 1 (-35 and -10 regions) and in blue the Promotor 2 (-35 and -10 regions).

2. Determination of alterations in ATL protein sequence

The *atl* nucleotide sequence of each strain was translated into the corresponding peptide sequence using Expasy Translate tool, and aligned with CLUSTAL Omega software (Figure 9).

In accordance with the differences identified in the nucleotide sequences, the ATL amino acid sequence of UAMS-1 strain was the one that showed less identity to COL, as well as to the other strains. Interestingly, for UAMS-1, most amino acid substitutions occurred in the region corresponding to the pro-peptide (PP). UAMS-1 has one insertion of 9 nucleotides which leads to an insertion of 3 amino acids (KPS) to the protein in the catalytic domain of AM.

The ATL sequence of strain HDE288 showed 5 specific amino acid substitutions, two in the pro-peptide and the one in the R1 repeat, and 8 residues deletion in the PP. The sequence of JE2 showed 5 specific amino acid substitutions, two in the R1 repeat, two in the R2 repeat and the other in the GL domain. Regarding strain WIS, the ATL protein sequence was identical to strain COL, since the two SNPs did not alter the peptide sequence. For strains NCTC8325 and MW2, the ATL sequence was more conserved in comparison to COL: the moderate number of SNP's observed in the gene

sequence (4 and 6, respectively), resulted in a total of 6 amino acid substitutions, distributed among the PP, AM domain, repeats R3 and GL domain.

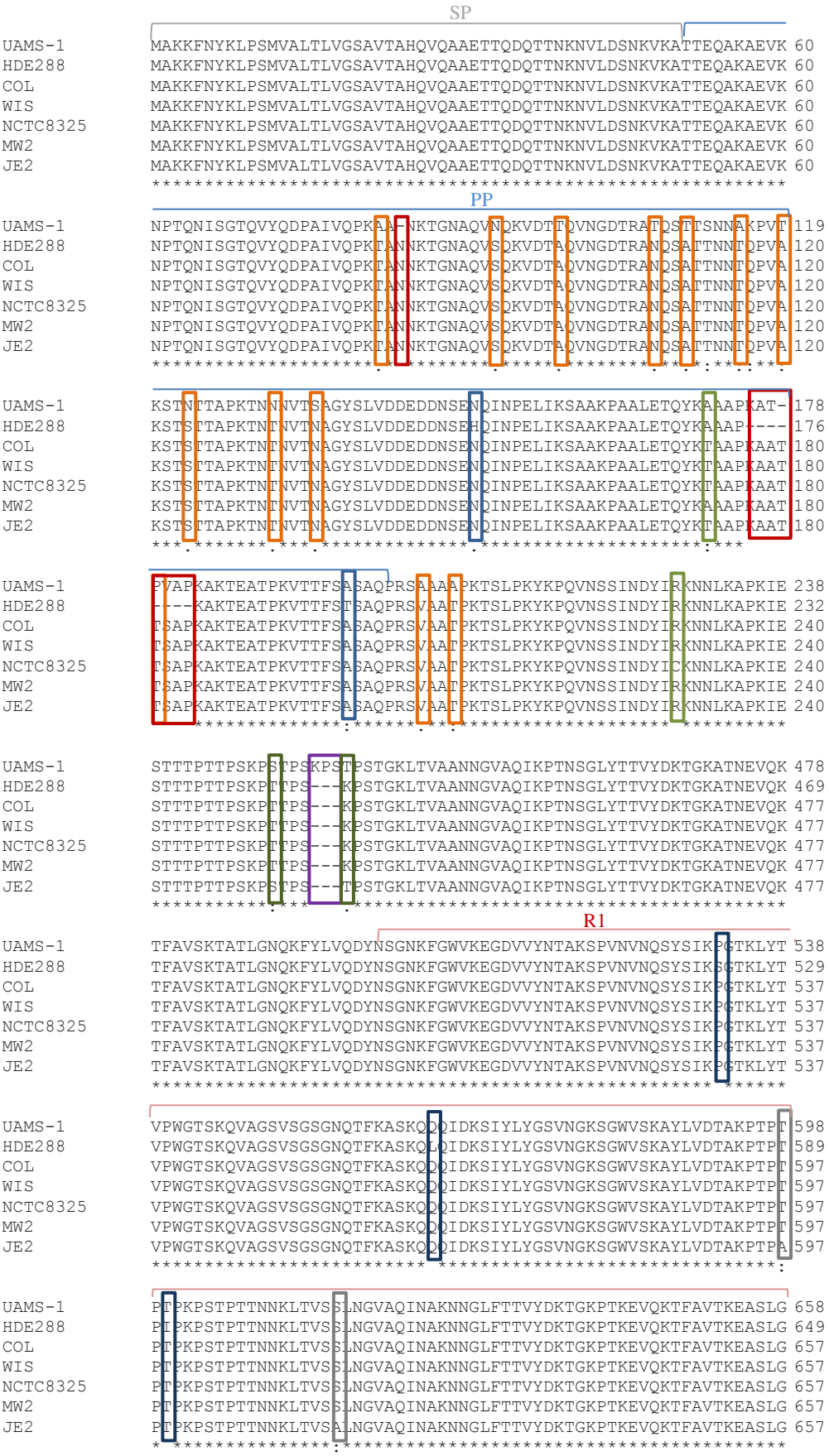
SP
PP
R1
UAMS-1
HDE288
COL
WIS
NCTC8325
MW2
JE2

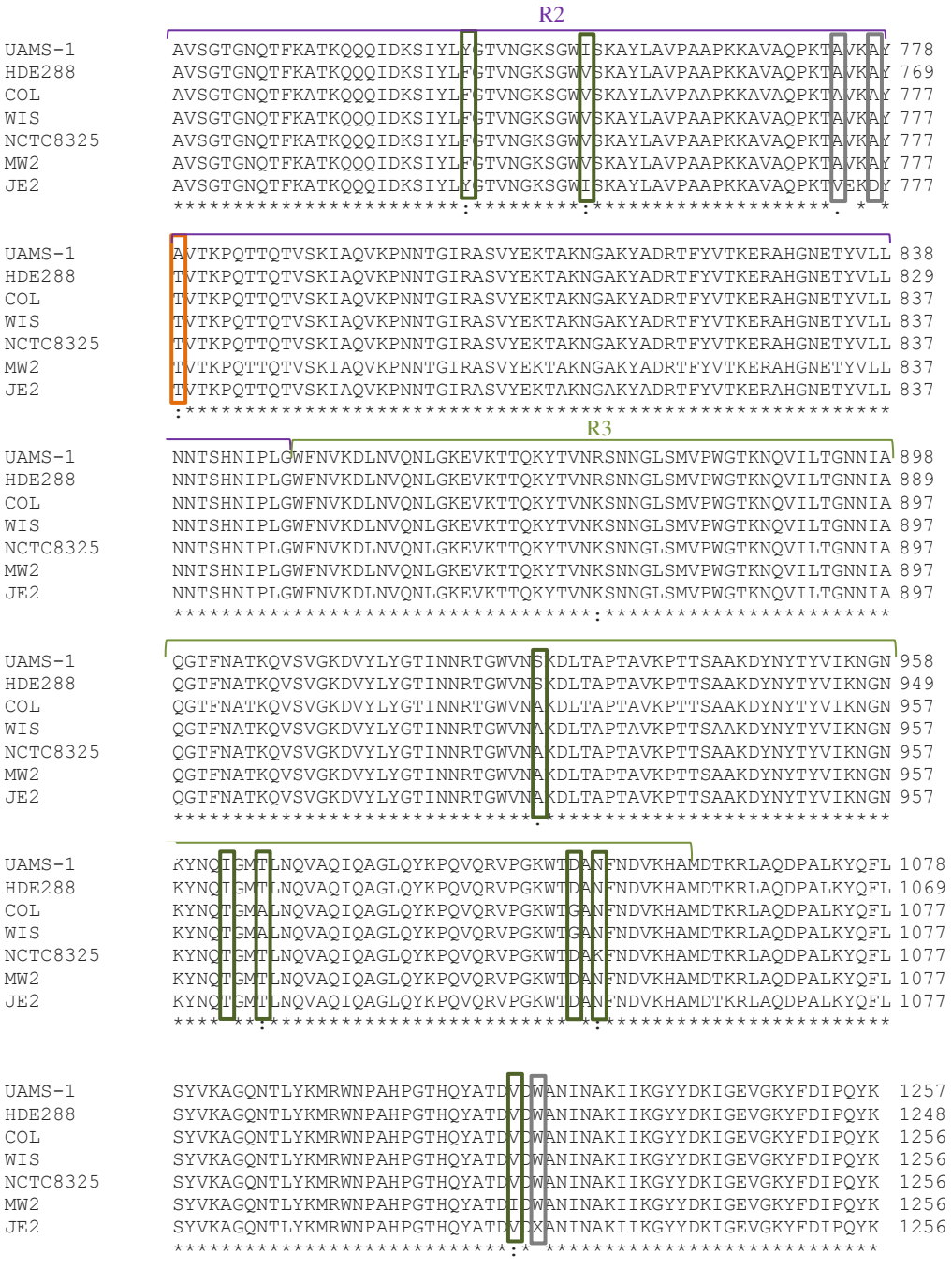

Figure 9 - Alignment of the amino acid sequence of ATL of *S. aureus* strains UAMS-1, HDE288, COL, WIS, MW2, NCTC8325 and JE2 (CLUSTAL Omega). In red are highlighted the amino acid deletions, in purple the insertions. Regarding amino acid substitutions, in orange are highlighted UAMS-1, in purple are JE2. In blue are HDE288 and the remaining strains in green.

Table 5 – SNP's, insertions and deletions in the *atl* gene from strains used in this study, and amino acid substitutions observed.

	SNP's		Insertion		Delection	AA Substitution	
	Position	Substitution	Position	Nucleotide	Position	Position	
NTCT 8325	2039	C→T	-	-	-	230	R→C
	4424	G→A	-	-	-	1025	A→T
	4503	G→A	-	-	-	1051	G→D
	4510	C→A	-	-	-	1053	N→K
MW2	1868	A→G	-	-	-	173	T→A
	4424	G→A	-	-	-	1025	A→T
	4503	G→A	-	-	-	1051	G→D
	5027	G→A	-	-	-	1126	V→I
UAMS-1 (SNP's >100 but only 24 cause amino acid substitution)	1595	A→G				82	T→A
					1660-1606	84	-
	1629	G→A				93	S→N
	1646	G→A				99	A→T
	1674	A→C				108	N→T
	1682	G→A				111	A→T
	1697	A→G				116	T→A
	1702	G→A				120	A→T
	1709	G→A				125	S→N
	1746	C→A				133	T→N
	1889	A→C				137	N→S
	1892	A→G				174	T→A
	1895	G→A				179	A→T
	-	-			1893-1894	180	-
	1896	A→C				181	T→P
	-	-			1897	182	S→V
	1968	T→C				206	V→A
	2008	A→G				209	T→A
	2140	A→T				252	T→S
	2329	A→C				256	K→T
	3576	T→A				742	F→Y
	4162	G→T				752	V→I

	4221 4416 4424	A→G G→A G→A				778 1022 1025 1051	T→A T→I A→T G→D
			2659	ACCATCAAC	-	255	KPS
WIS	1109	A→G	-	-	-	-	-
	1197	G→A	-	-	-	-	-
HDE288	1802	A→C	-	-	-	152	N→H
	1868	A→G				174	T→A
			-	-	1868-1992	176-184	-
	1946	G→A				199	T→A
	2942	C→T	-	-	-	531	P→S
	3042	A→T	-	-	-	563	Q→L
	3147	C→T	-	-	-	599	T→I
	3802	A→G	-	-	-	874	K→R
	4133	G→T	-	-	-	928	A→S
	4416	C→T	-	-	-	1022	T→I
	4424	G→A	-	-	-	1025	A→T
	4503	G→A	-	-	-	1051	G→D
JE2			1071	G	-	-	-
	2619	C→G	-	-	-	252	T→S
	2686	T→A	-	-	-	256	K→T
	2743	A→T	-	-	-	597	T→A
	2942	C→T	-	-	-	615	S→A
	2998	T→C	-	-	-	742	F→Y
	3042	A→T	-	-	-	752	V→I
	3147	C→T	-	-	-	773	A→V
	4156	T→C	-	-	-	776	A→D
	4424	G→A	-	-	-	1025	A→T
	4503	G→A	-	-	-	1051	G→D

3. ATL protein expression along growth

In order to analyze the ATL protein expression over time and to determine if the expression pattern and the proteolytic profile varies from strain to strain, the relative amount of AM and GL was assessed by Western blotting, for strains COL, NCTC 8328, WIS, HDE288, JE2, UAMS-1 and MW2. Western blotting (or protein immunoblot) is an analytical technique that can be used to detect specific proteins in a complex extract, using specific antibodies. We used the previously available anti-GL and anti-AM raised antibodies raised against proteins GL-C (GL without repeats domain) and ATL-H (AM without repeats domain) respectively (Grilo *et al,* unpublished). The amount of ATL protein was assessed in the cell supernatant fraction (spent medium) (Figure 11, panel A) and also in the cell wall fraction (Figure 11, panel B).

Culture samples were taken at discrete time points along the growth curve (Figure 10).

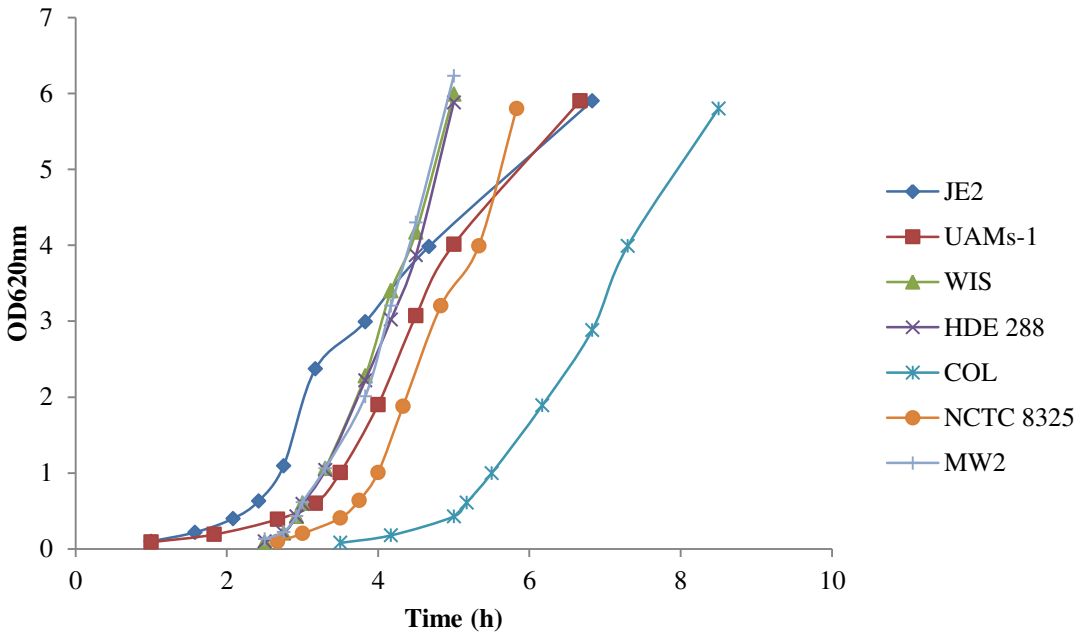

Figure 10 – Growth curve of strains COL, WIS, HDE288, UAMS-1, JE2, NCTC8325 and MW2 in complex medium at 37ºC.

3.1.Expression analysis using anti-GL antibody

The protein extracts were separated by SDS-PAGE and transferred to a nitrocellulose membrane that was then hybridized with the anti-GL antibody. By analyzing the apparent molecular weight of the bands obtained, the anti-GL antibody was observed to hybridize with the full ATL protein (137.5 kDa), the ATL without the PP (121 kDa) and also with more than one processed form of the GL domain, the full form R3GL (53.6 kDa), and GL (40.5 kDa).

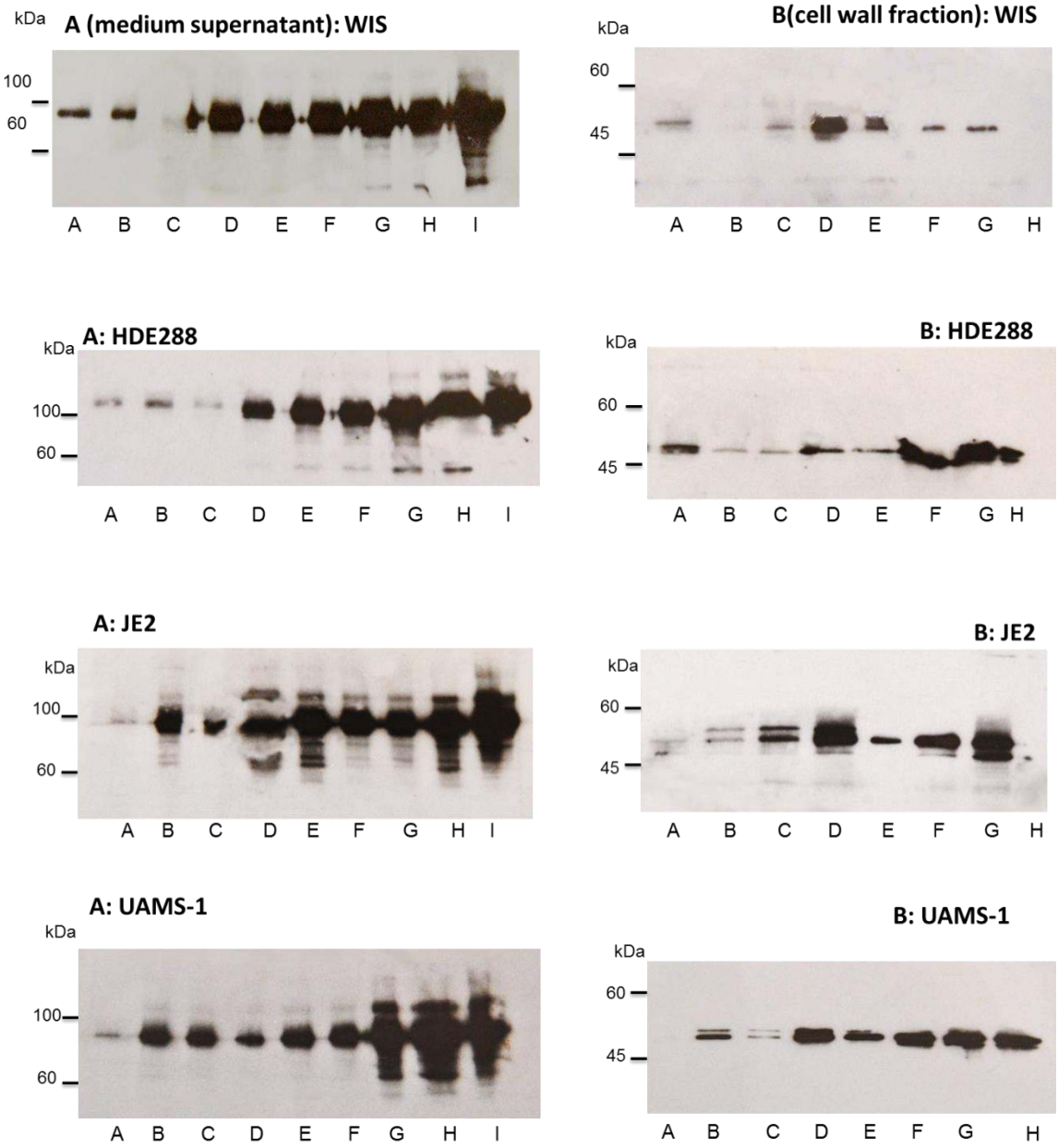

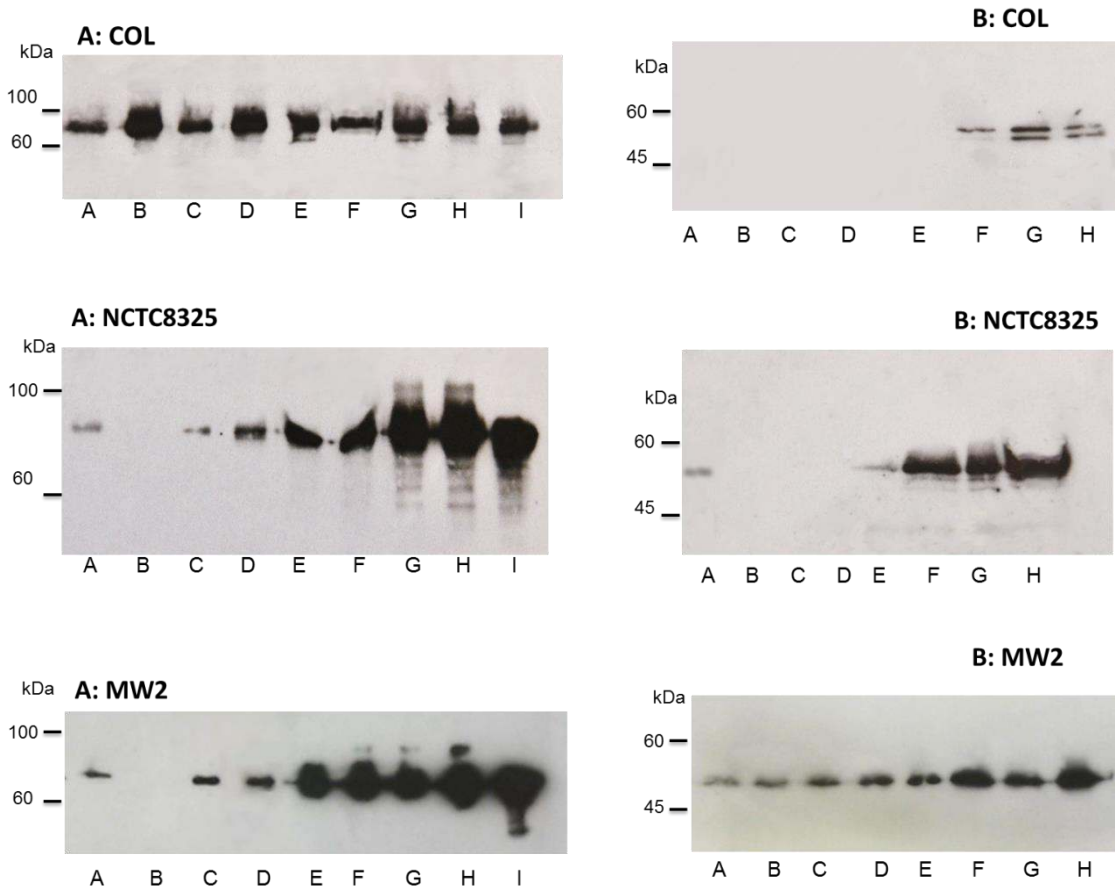

Figure 11 – GL expression along time. Western blotting was performed for protein extracts from strains WIS, HDE288, JE2, UAMS-1, COL, NCTC8325 and MW2, using anti-GL specific antibody. (A) Cell supernatant; (B) Cell wall fraction. A- OD 0.2, B- OD 0.4, C- OD 0.6, D- OD 1, E- OD 2, F- OD 3, G- OD 4, H- OD 6, I- OD 11.

Differences not only in the amount of ATL protein produced along time, but also in the number and molecular weight of the protein bands obtained, were observed between the 7 strains analyzed.

Overall, for most strains, ATL protein (the unprocessed form or the AM-R1R2R3-GL form) seemed to accumulate firstly in the supernatant (at OD~0.2-0.4) and only later was the processed GL domain targeted to the cell wall (starting at OD~0.4).

WIS, HDE 288, JE2, UAMS-1, NCTC 8325 and MW2 showed a similar ATL expression pattern in the supernatant, with a gradual increase along time, while COL showed a constant ATL expression pattern. The ATL unprocessed form and the AM-

R1R2R3-GL form were not observed in the cell wall fraction for the period of growth analyzed.

Regarding GL domain, several processed forms accumulated together with the ATL full protein in the supernatant of most strains except COL. For strains HDE288 and JE2, GL domain began to accumulate in the supernatant during exponential phase (OD-0.1) and later (OD-4) for strains WIS, UAMS-1 and NCTC8325. For strain MW2, GL domain was only detected during late stationary phase (OD-11). At the cell wall level, GL domain was present in one single form (corresponding to one band) for strains HDE288 and MW2 or as several processed bands (corresponding to multiple bands) for strains WIS, JE2, UAMS-1, COL and NCTC8325. These distinct GL bands may correspond to different cleavage events of GL protein.

Regarding the amount of GL domain present in the cell wall fraction, it was interesting to observe three different patterns: for strains WIS, HDE288, JE2 and UAMS-1, GL domain showed an accumulation peak at exponential phase (OD-1) followed by a rapid decrease at OD-2 and finally a steady increase; for strains COL and NCTC8325, GL domain only started to accumulate at late exponential phase (OD~3-4), while for strain MW2, it constantly accumulated along time.

3.2. Expression analysis using anti-AM antibody

The same protein extracts were separated in SDS-PAGE and transferred to a new nitrocellulose membrane that was hybridized with anti-AM antibody. By analyzing the apparent molecular weight of the bands obtained, we observed that the anti-AM antibody was not able to recognize the unprocessed form of ATL (137.5 KDa), only the AM domain (63.3 kDa). The Western blotting results are shown in Figure 12, panel A (supernatant fraction) and panel B (cell wall fraction).

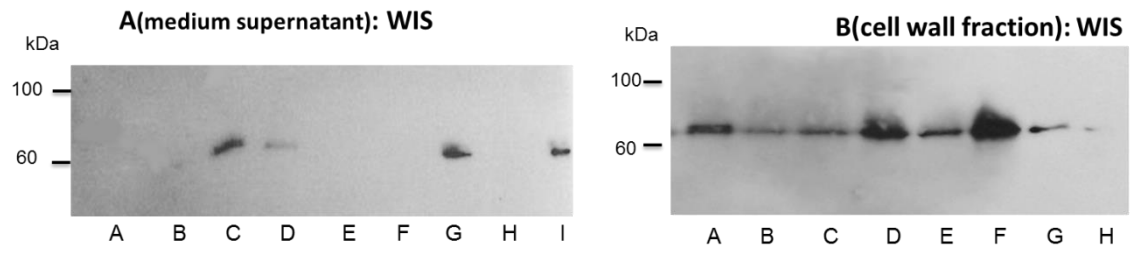

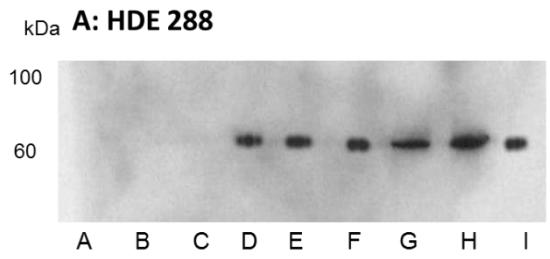
kDa
A: HDE 288
100
60
A B C D E F G H I

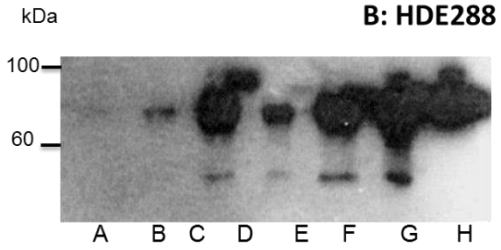
kDa
B: HDE288
100
60
A B C D E F G H

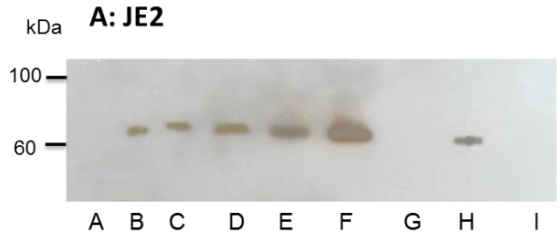
kDa
A: JE2
100
60
A B C D E F G H I

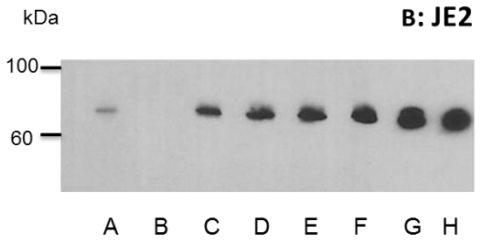
kDa
B: JE2
100
60
A B C D E F G H

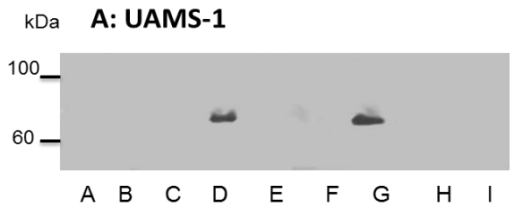
kDa
A: UAMS-1
100
60
A B C D E F G H I

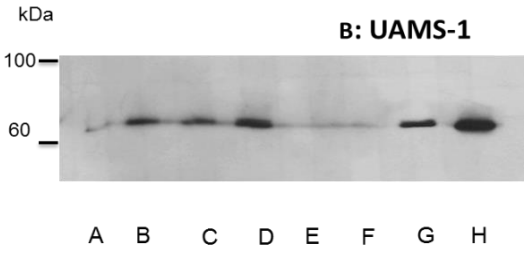
kDa
B: UAMS-1
100
60
A B C D E F G H

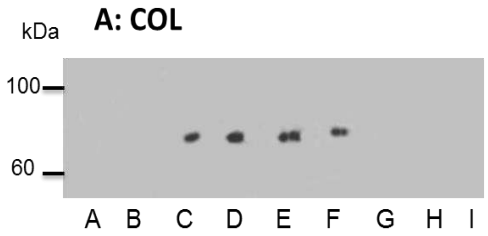
kDa
A: COL
100
60
A B C D E F G H I


kDa
B: COL
100
60
A B C D E F G H

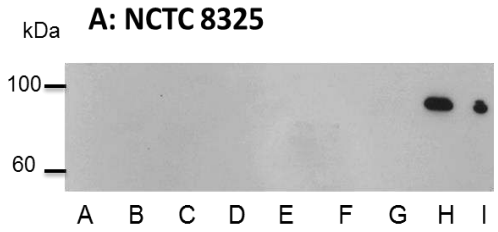
kDa
A: NCTC 8325
100
60
A B C D E F G H I

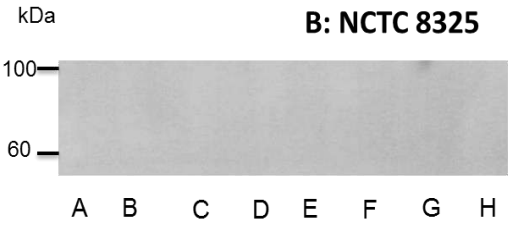
kDa
B: NCTC 8325
100
60
A B C D E F G H

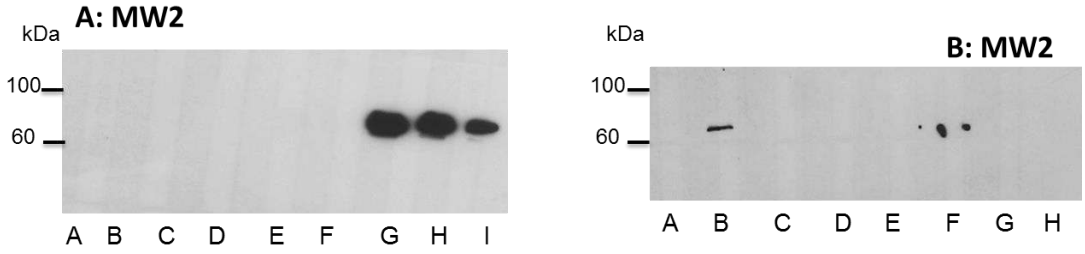

Figure 12 – AM expression along time. Western blotting was performed for protein extracts from strains WIS, HDE288, JE2, UAMS-1, COL, NCTC8325 and MW2, using anti-AM specific antibody. (A) Cell supernatant; (B) Cell wall fraction. A- OD 0.2, B- OD 0.4, C- OD 0.6, D- OD 1, E- OD 2, F- OD 3, G- OD 4, H- OD 6, I- OD 11.

Differences in the expression pattern of AM domain along time and amongst strains was even more striking than for GL domain.

While WIS, COL and UAMS-1 showed low and poorly consistent amounts of AM in the supernatant, NCTC8325 and MW2 only showed AM presence at late stationary phase (OD 6 to 11). HDE288 did not present AM in the supernatant until late exponential phase (OD 1), and JE2 did not present AM in the supernatant in the stationary phase.

Regarding the amount of AM domain present in the cell wall fraction, it was interesting to observe, as for GL domain, three different patterns: for strains WIS, HDE288 and UAMS-1, AM domain showed an accumulation peak at exponential phase (OD-1) followed by a rapid decrease at OD-2 and finally a steady increase; for strains COL, NCTC8325 and MW2, AM domain did not accumulate at the cell wall fraction; for strain JE2, it constantly accumulated along time.

4. The association between DNA and GL lytic activity

The interaction between DNA and GL seems to have an important role in the biofilm formation. In order to understand if the GL-DNA association also has importance in lytic activity, lytic assays were performed using heat-inactivated cells, cell wall fraction and purified peptidoglycan as substrate for GL in the presence of added DNA. To determine if the cell wall or the peptidoglycan composition of the strain would influence GL activity, these were tested for all the strains under study.

ATL-C recombinant His-tagged protein (GL domain without the repeat region) was expressed for the digestion assays, and then purified using a Ni-NTA column. The Ni-NTA (nickel nitrile-triacetic acid) column co-purification is based in the high affinity between polyhistidine tagged proteins and the nickel ions present in the matrix of the Ni-NTA columns. Proteins bound to the resin are eluted by competition with imidazole.

The protein purity level was verified by SDS-PAGE as shown at figure 13.

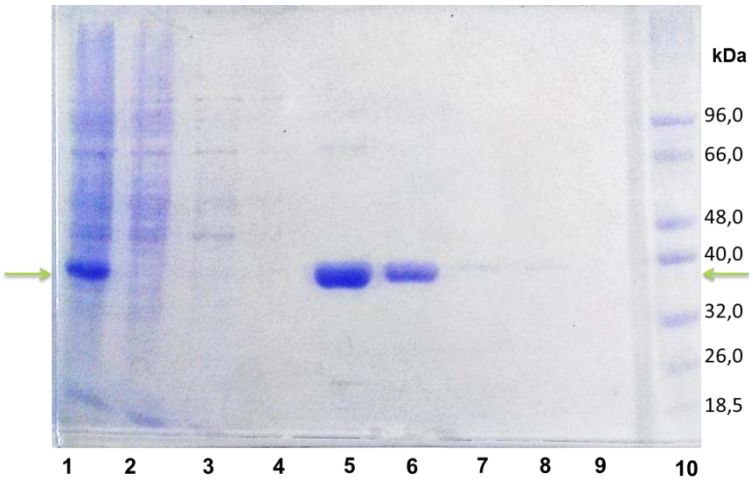

Figure 13 - Purification of ATL-C recombinant His-tagged protein. Lane 1: total extraction lysate; Lane 2: flow-through; Lane 3 and 4: washes; Lane 5-9: elutions 1-5; Lane 10: protein marker (Low Molecular Weight Protein Marker). Green arrows: ATL-C (GL without R3).

In order to define the best lytic activity conditions, different buffers were tested (Sodium Phosphate Buffer pH 7.4; Sodium Phosphate Buffer pH 5.5; Tris-HCl pH 8; Tris-HCl pH 7.4; Tris-HCl pH 5.5) and different GL protein concentrations (5ng/µl; 10ng/µl; 20ng/µl). The reaction conditions that retrieved higher GL peptidoglycan lytic activity levels were buffer Tris pH 7.5 and a protein concentration of 5ng/µl. The sample was incubated at 37ºC with agitation and the OD_{600} was monitorized for 2h with 5 minute intervals reads.

As positive controls, mutanolysin (a muralytic enzyme that cleaves the N-acetylmuramyl-β-N-acetylglucosamine linkage of the bacterial cell wall polymer peptidoglycan-polysaccharide) and lysostaphin (enzyme that cleaves the crosslinking pentaglycin bridges of *S. aureus* peptidoglycan) were used; both enzymes were able to

degrade the heat-inactivated cells, the cell wall fraction and the purified peptidoglycan samples. To determine if the salmon sperm DNA added to the samples would influence the measurements, controls were performed only with substrate and added DNA; no significant differences were observed when compared to the samples without DNA.

Differences were observed in the lytic activity of GL when using substrates from different strains: purified peptidoglycan, cell wall and heat-inactivated cells (Figure 14). The following graphics are presented with representative values of time, the graphics with all time points are presented in annex 2.

The lytic activity of GL was higher for the peptidoglycan of strains WIS, HDE288, UAMS-1 and MW2. In WIS and MW2 GL-DNA with 0.05 and 0.5 mg/mL, respectively, has a higher digestion of peptidoglycan.

Regarding the cell wall, it is observed more lytic activity of GL in the strains HDE288 and MW2. There seems to be no significant difference in GL activity when associated with DNA.

In the inactivated cells there is a gradual decrease in OD_{600} when GL is added, however no differences are observed in the presence of DNA.

GL showed no lytic activity for the heat-inactivated cells of all seven strains. Furthermore, GL also did not show lytic activity for the cell fraction or the purified peptidoglycan of strain COL. The lytic activity of GL was higher for the cell wall fraction of strains MW2 and HDE288; accordingly, for their peptidoglycan fraction as well. For all other strains (WIS, UAMS-1, JE2 and NCTC8325), GL only showed lytic activity in the peptidoglycan fraction.

Regarding the effect of DNA addition to the lysis reaction, contrary effects were observed for the lytic activity of GL against WIS and MW2 peptidoglycan: the 0.05 mg/ml concentration was found to activate GL lytic activity on WIS peptidoglycan and inhibit the same activity on MW2 peptidoglycan. In contrast, the higher DNA concentration, 0.5 mg/mL, was responsible for inhibiting GL activity on WIS peptidoglycan and activates it on MW2 peptidoglycan.

(A) COL

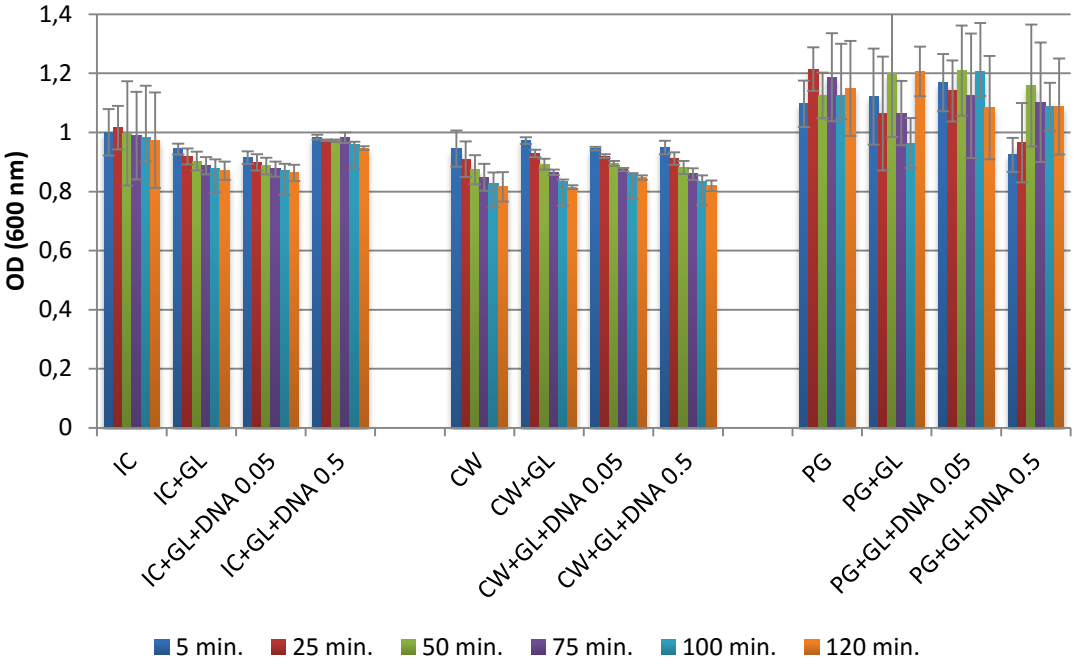
OD (600 nm)
1,4
1,2
1
0,8
0,6
0,4
0,2
0
IC
IC+GL
IC+GL+DNA 0.05
IC+GL+DNA 0.5
CW
CW+GL
CW+GL+DNA 0.05
CW+GL+DNA 0.5
PG
PG+GL
PG+GL+DNA 0.05
PG+GL+DNA 0.5
5 min.
25 min.
50 min.
75 min.
100 min.
120 min.

(B) WIS

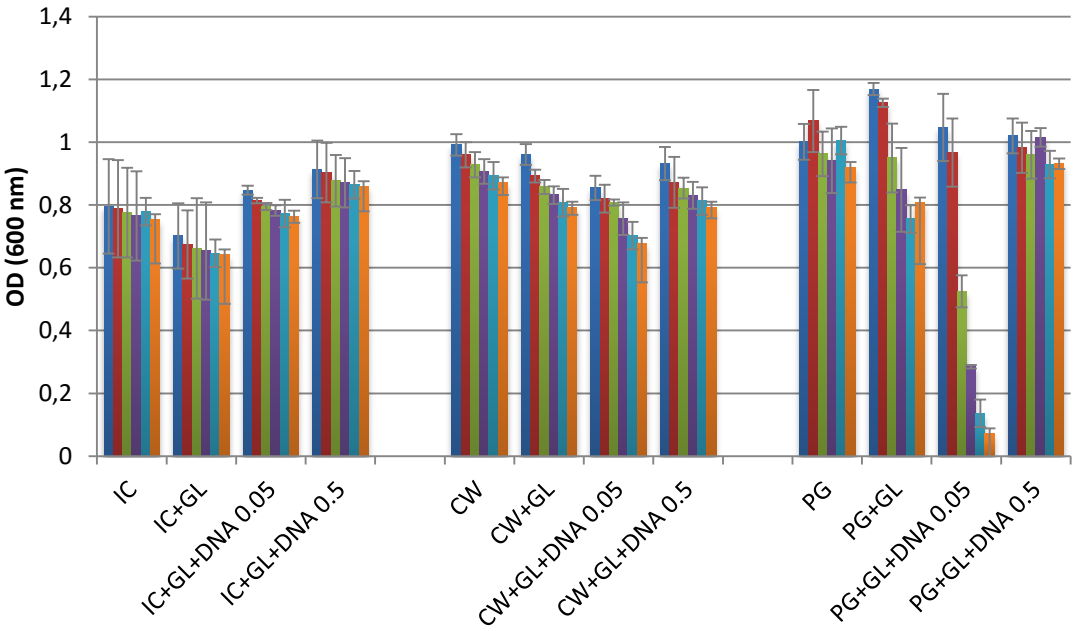
OD (600 nm)
1,4
1,2
1
0,8
0,6
0,4
0,2
0
IC
IC+GL
IC+GL+DNA 0.05
IC+GL+DNA 0.5
CW
CW+GL
CW+GL+DNA 0.05
CW+GL+DNA 0.5
PG
PG+GL
PG+GL+DNA 0.05
PG+GL+DNA 0.5

(C) HDE288

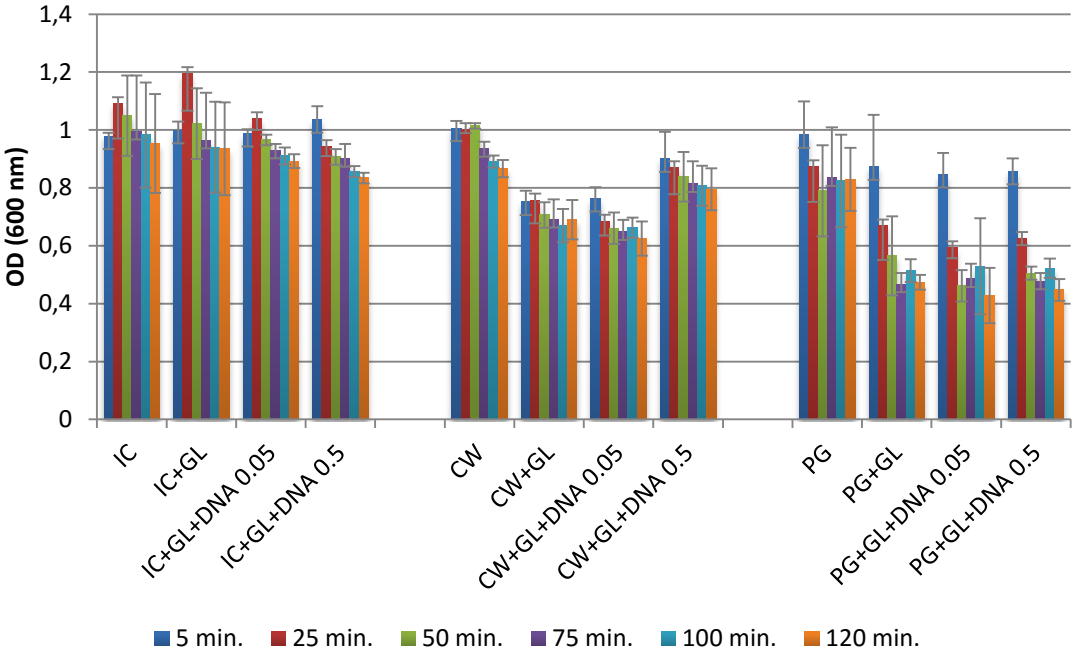

(D) UAMS-1

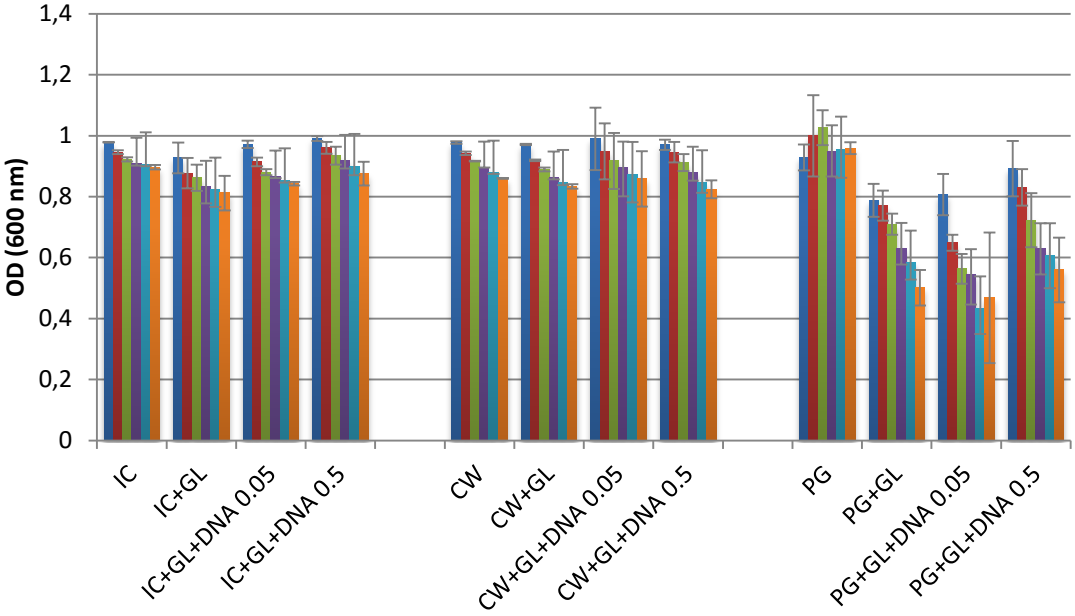

(E) JE2

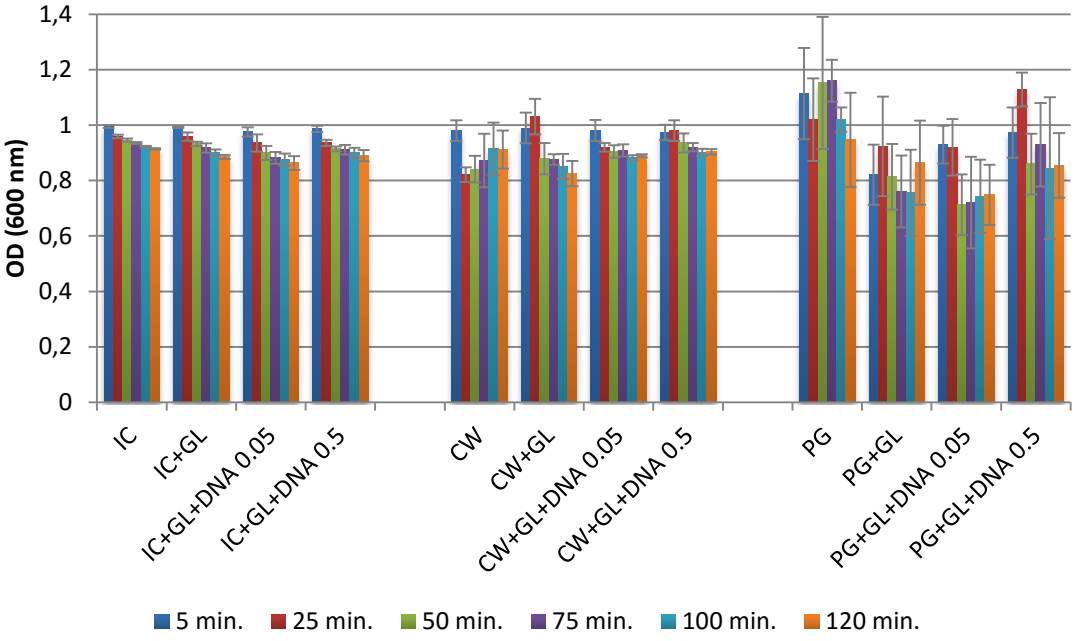

(F) NCTC8325

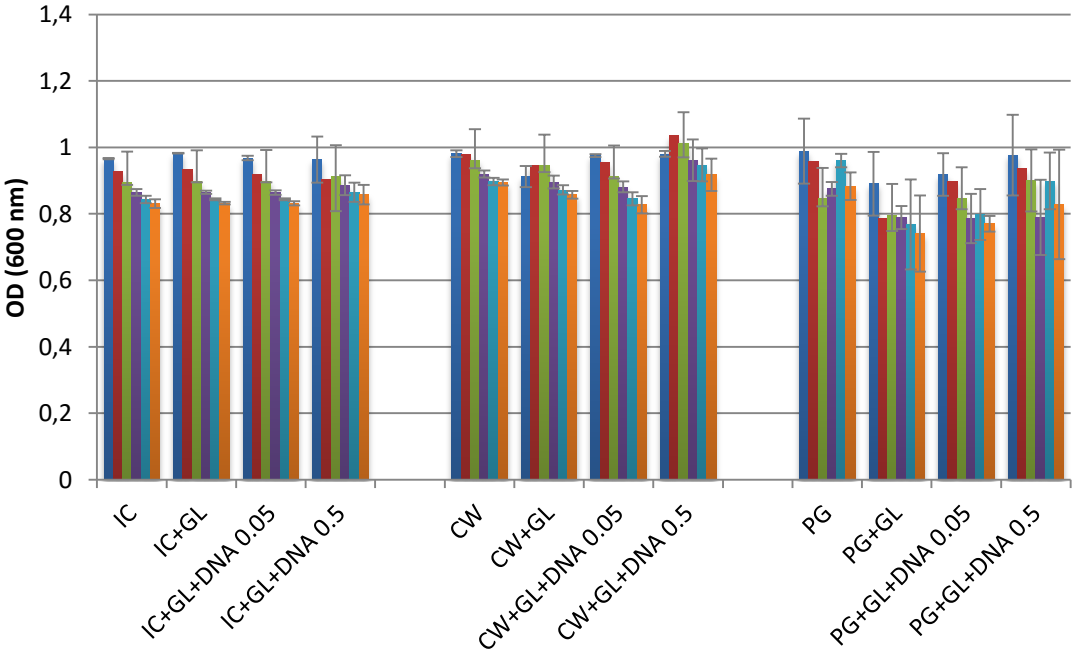

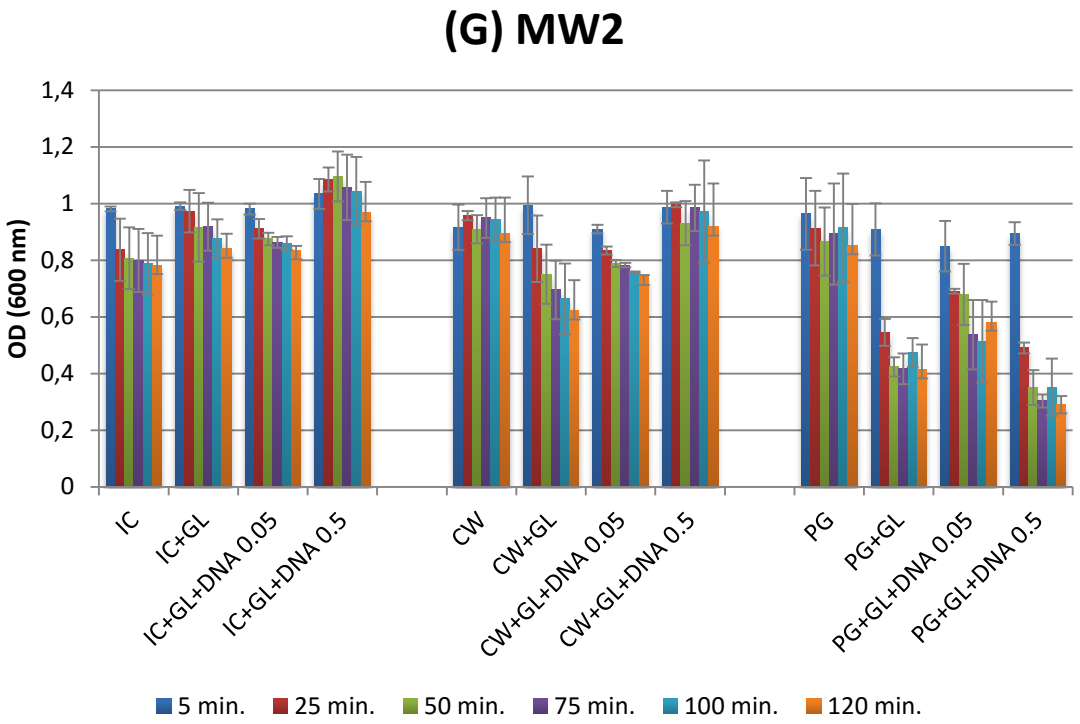

Figure 14 – Lytic activity of GL protein and DNA-GL association in (A) COL; (B) WIS; (C) HDE288; (D) UAMS-1; (E) JE2; (F) NCTC8325; (G) MW2, when studied in heat inactivated cells (IC); cell wall (CW), and peptidoglycan (PG), along time.

5. Expression of ATL-C protein in Minimum medium for NMR analysis

In order to express and purify GL for NMR characterization, ATL-C protein (GL without repeat domain) was expressed in Minimum medium, in different volumes, and then purified using the manual Ni-NTA column.

The protein purity level was verified by SDS-PAGE as showed at figure 15.

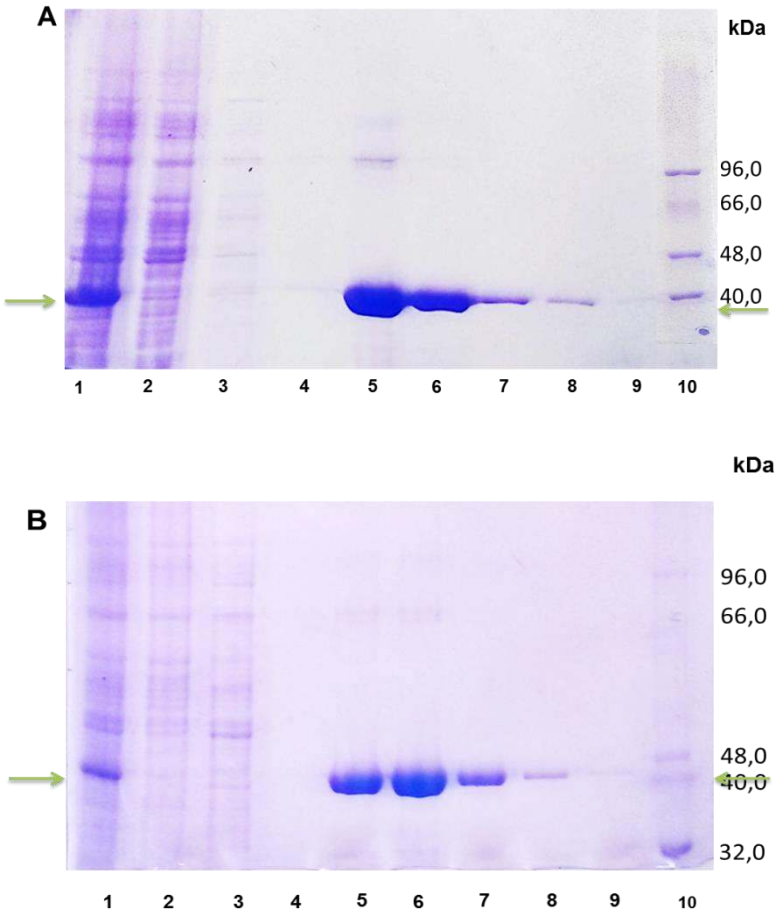

Figure 15 – (A) Purification of ATL-C 200mL. (B) Purification of ATL-C 1L. Lane 1: lysate total extraction; Lane 2: flow through; Lane 3 and 4: washes; Lane 5-9: Elutions 1-5; Lane 10: protein marker (Low Molecular Weight Protein Marker). Green arrows: ATL-C (GL without R3).

Under complete denaturing conditions, proteins migrate through an electric filed according to their molecular weight. When a protein has not been completely denatured and forms a dimeric structure an extra band appears in the SDS-PAGE, with the double value of its molecular weight. As the protein is completely denatured and not dimerized, this extra band didn't appear.

As shown in the gels above, the protein has expressed in minimum medium, so it was possible to continue with the same protocol in labeled minimum medium (^{15}N) (Figure 16).

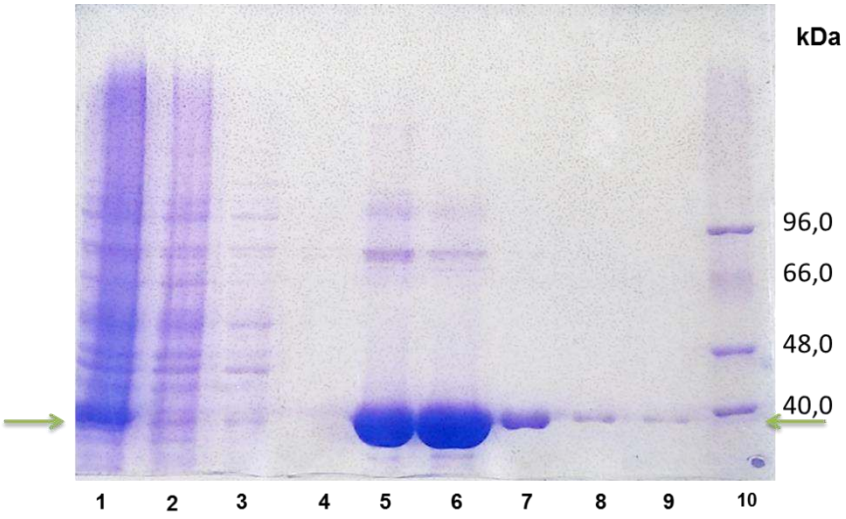

Figure 16 – Purification of ATL-C 500mL ^{15}N minimum medium. Lane 1: lysate total extraction; Lane 2: flow through; Lane 3 and 4: washes; Lane 5-9: Elutions 1-5; Lane 10: protein marker (Low Molecular Weight Protein Marker). Green arrows: ATL-C (GL without R3).

6. NMR analysis

In structural biology it is necessary to efficiently screen for the optimal conditions to obtain stable protein that can subjected to subsequent structure determination. In a globular folded protein the individual residues are packed into chemical environments, which are very different from the random coil situation.

The HSQC-NMR spectrum of an unfolded protein is the sum of the random coil spectra of the amino acid residues in the proteins.

In a HSQC-NMR spectrum of a folded protein the dispersion of signals is far beyond the envelope of signals seen in the spectrum of the unfolded protein, reflecting that nuclei in the folded form are subject to many different types of microenvironments of chemical screens.

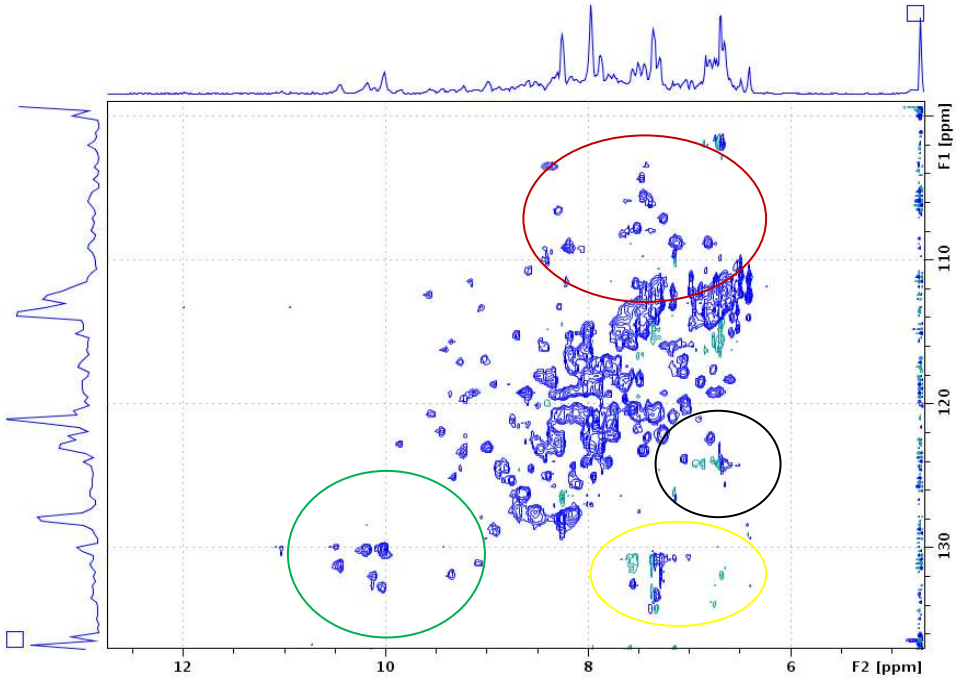

Figure 17 – ^{15}N-HSQC spectrum 2D of GL domain in 25mM Tris-DCL and 75mM NaCl. Red circle: Asn and Gln groups; green circle: Trp groups; black circle: C-terminal groups; yellow circle: Arg groups.

In the GL ^{15}N-HSQC spectrum (Figure 17) we can observe a dispersion in the frequencies of the resonances, which demonstrates that the protein is folded. We can also observe the Asn and Gln side chain NH_2 group peaks at the superior part of the spectrum (mark as red), the Trp side chain Hε-Hε on the left bottom (mark as green), the Arg side chain Hε-Nε on the right bottom (mark as yellow) and the C-terminal amino acid (mark as black).

Chapter IV – Discussion and Conclusions

The main objective of this project was to characterize the ATL protein regarding strain specificity. For this purpose, four tasks were proposed: (i) study the different processed forms and the cell compartment where the cleavage occurs, in different *S. aureus* backgrounds; (ii) analyze the expression of ATL along time in the different strains; (iii) analyze the impact of DNA on GL lytic activity on the peptidoglycan of several *S. aureus* lineages; (iv) characterize GL-DNA interaction by NMR.

Staphylococcus aureus is a very clonal microorganism that is able to disseminate worldwide. Among the several clonal lineages of *S. aureus*, in this study we included strains representing MSSA, CA-MRSA and HA-MRSA clonal lineages that showed different ATL-dependent biofilm formation patterns.

COL is a hospital acquired MRSA with a *sccmec* type I, member of the "archaic" clone of MRSA and perhaps the most studied MRSA strain. COL was isolated from a patient in Colindale, United Kingdom in 1960 (Jevons, 1961). This strain is a member of the most successful of all MRSA lineages, which nowadays not only includes hospital but also community-associated strains. NCTC 8325 and UAMS-1 are both MSSA; NCTC 8325 was isolated from a corneal ulcer, and the original genome map of *S. aureus* was based on this strain (Novick, 1991), UAMS-1 was isolated from an osteomyelitis patient. MW2, a community acquired MRSA with *sccmec* type IV, was isolated in 1998 in the USA and caused fatal septicemia and septic arthritis (Baba, 2002). It belongs to the USA400 clone, one of the most common lineages in the United States. WIS is a CA-MRSA with *sccmec* type V, isolated in Taiwan. HDE288 is a HA-MRSA with *sccmec* type VI, a pediatric clone isolated in Nicaragua. JE2 is a CA-MRSA that belongs to USA300 clone, isolated from skin and soft tissue infections in USA.

1. *atl* gene SNPs affect the protein sequence

Single nucleotide polymorphisms, frequently called SNPs, are the most common type of genetic variation. SNPs within a coding sequence do not necessarily change the amino acid sequence of the protein.

The SNPs observed in the *atl* region of the strains in this study provided interesting information. No alterations were observed in the promotor region, indicating that any expression differences between the strains do not result from mutations in this region. Some SNPs resulted in amino acid residue substitutions and only one was located in the vicinity of the active site of GL domain, E1128 (V1126I) in MW2 strain. The sequence of ATL protein of UAMS-1 showed more differences, mainly in the propeptide region, when compared with the other strains, suggesting an altered proteolytic cleavage pattern. The ATL sequence of HDE288 and JE2 also showed several amino acid substitutions, more dispersed along the ATL protein domains (PP, AM, R repeats and GL). The only ATL sequence that was identical to COL was the one of WIS strain.

2. Differences in the expression of ATL protein along growth

ATL is 137.5 kDa murein hydrolase, with two catalytic domains: AM (63.3 kDa), that contains an enzymatic domain and two repeat domains (R1 and R2), and GL (53.6 kDa), containing an enzymatic domain and a single repeat domain (R3).

To analyze the ATL protein expression over time and determine if the expression pattern varies from strain to strain, the relative amount of ATL was assessed by Western blotting, using specific antibodies against AM and GL domains. The anti-GL antibody was found to recognize the ATL complete protein while also recognizing GL domain. At the beginning of exponential phase, ATL protein was present only in the supernatant, suggesting that the protein accumulated in the cell exterior and only after a protein treshold limit it was then targeted to the cell wall, already in a cleaved form. The complete form of ATL (137 kDa) was not present in the cell wall fraction.

The presence of GL was more evident in the pellet, suggesting that after cleavage, GL domain is targeted to the cell wall. These results support the recently described function for this hydrolase in biofilm development: GL may provide an attachment point between the cell surface and the biofilm matrix.

Regarding AM domain, COL and NCTC8325 strains seem not to target AM domain to the cell wall. However, presence of AM at the cell wall was observed in the other strains, in accordance with the literature description of R1R2 repeats being responsible

for targeting AM domain to the pellet (Biswas, 2006; Marino *et al*, 2002). These observations demonstrate how different strains can have different levels of AM associated to the cell wall and raise two hypotheses: AM is not located at the cell wall in some strains, or AM is only targeted to the cell wall at a later growth phase. Two possible mechanisms are described for the specific localization of ATL at the septal sites of the cell surface. One is that ATL protein is synthesized, translocated at the cell division site, and localized with an anchoring component. The other is that ATL is secreted into the culture medium and reabsorbed to an anchoring component via ligand-receptor interaction (Schlag *et al*, 2010; Yamada *et al*, 1995). Differences in the structure of the repeat domains of AM and GL might reflect the differences of the recognition sites on staphylococcal cell walls. Our results confirm that targeting of AM and GL occurs through independent mechanisms: GL was present in the cell wall of all strains, in contrast to AM. Furthermore, the fact that no AM was observed in the cell wall of some strains strengthens the second hypothesis that the ATL domains are secreted and subsequently reabsorbed.

Different ATL, GL and AM expression patterns along the growth curve were observed for the different strains and also distinct proteolytic patterns, illustrated by the occurrence of bands of different sizes. However, no direct relation with the amino acid substitutions identified previously was possible to establish. For example, the ATL sequence of WIS and COL strains are identical, however, their ATL, GL and AM expression profiles were completely distinct.

3. The impact of DNA on GL lytic activity

ATL is the most predominant peptidoglycan hydrolase in staphylococci. Although several studies have focused on the function of ATL, the individual contributions of the AM and GL domains are not known. Recent studies reveal the importance of the interaction between DNA and GL in biofilm formation. This fact raises the question if the interaction between DNA and GL may also be important for the major function of ATL, the peptidoglycan lytic activity.

The results obtained showed no significant differences in the lytic activity of GL when DNA is added, except for strains WIS and MW2. The effect of both DNA concentrations on the lytic activity of GL for the peptidoglycan of these two strains, was contradictory: it had apposite inhibitory and activating effects. Differences in the peptidoglycan composition of these strains may explain the different lytic activity of GL protein and the peptidoglycan of these strains should be analyzed in future experiments. Furthermore, all the assays were performed with GL protein from COL strain. It is interesting to observe no lytic effect against COL inactivated cells, cell wall or even peptidoglycan, suggesting that GL may act as a weapon against other *S. aureus* strains, although not having lytic activity against its own surface polymers.

Regarding the heat-inactivated cells, no effect of GL lytic activity was observed; as GL is expected to lyse the peptidoglycan mesh at discrete locations, this behavior was expected. Also, other cell surface associated factors/enzymes may also bind to DNA, in this way competing with GL. Concerning the results for the cell wall fraction, the presence of WTAs, which prevents *S. aureus* from autolysis (Schlag *et al*, 2010), can be, also, the explanation to the non-significant lytic activity. It is believed that targeting of amidase R1R2 repeat domains is rather based on an avoidance strategy by WTA, which prevents binding of ATL. As WTAs are abundant in the old cell wall but not at the cross-wall region, ATL can bind to the septal region.

It would be interesting to analyze the lytic activity of AM-R1R2 in these strains, in the presence of added DNA, since the DNA-binding activity of the AM domain appears to be restricted to the repeats (Grilo *et al*, 2014).

4. NMR

Nuclear magnetic resonance (NMR) spectroscopy is a methodology that reveals the atomic structure of macromolecules in solution in highly concentrated samples (approx. 1 mM) (Bharti and Roy, 2012). The technique is based on the fact that certain atomic nuclei are intrinsically magnetic. Only a limited number of isotopes display this property, called spin (½), such as ^{1}H, ^{15}N, ^{13}C. A spinning protein in α state can be raised to an excited state (β state) applying a pulse electromagnetic radiation (a radio-

frequency). The spin will change from α to β and resonance will be obtained. A resonance spectrum for a molecule can be obtained varying the magnetic field at a constant frequency of electromagnetic radiation or keeping the magnetic field constant varying electromagnetic radiation. With this technique, one, two and tree-dimension spectra (^{1}H-spectrum, ^{1}H-^{15}N-spectrum and ^{1}H^{15}N-^{13}C-spectrum) can be obtained in order to determine the protein structure (Montelione et al., 2000). To beat the low natural abundance of ^{15}N and ^{13}C for obtaining two and tree-dimension spectra, incorporation of such isotopes must be forced by expressing the protein in minimal media supplemented with the isotopes.

In this study, ATL-C, GL domain without repeats, was expressed in ^{15}N labeled minimal medium and then analyzed by NMR. The ^{15}N-HSQC spectrum obtained revealed that the protein is folded since a high signal dispersion is observed. These results provided important contributions for the characterization of GL by NMR. The structure of GL domain has not been elucidated yet, in contrast with AM domain. It is necessary in the future to optimize the conditions of the expression of GL to obtain a ^{13}C spectrum essential for the study of the interaction between GL and DNA.

5. Conclusion

This study allowed to identify distinct patterns of ATL protein expression and proteolytic cleavage that may be the basis for the primary phenotypic differences associated to ATL protein. GL and AM expression varies from strain to strain, and GL and AM were shown to be the targeted to the cell wall through different mechanisms. Our results support the hypothesis of ATL being secreted into the culture medium and then retargeted to the cell wall. The effect of DNA-GL binding in lytic activity of GL was found to be, as already observed for biofilm formation, strain dependent. The structural characterization of GL-DNA association may clarify the mechanisms behind these observations.

The hydrolysis of peptidoglycan by hydrolases results in a strong bactericidal effect which makes this group of enzymes an alternative antibacterial weapon, for example a

possible vaccination scheme with ATL-AM has been studied and this vaccine was shown to induce Th1 and Th2 immune response (Nair *et al*, 2015).

Due to the importance already demonstrated of the ATL in *Staphylococcus aureus* and the possibility of being a potential weapon against this microorganism, it is important to study and characterize this protein.

References

Abraham, E. P., and E. Chain. 1940. An Enzyme from Bacteria able to Destroy Penicillin. Nature, **146**:837.

Amako, K., and A. Umeda. 1977. Scanning electron micros-copy of *Staphylococcus*. Journal of Ultrastructure Research, **58**:34–40.

Archer, N. K., M. J. Mazaitis, J. W. Costerton, J. G. Leid, M. E. Powers, and M. E. Shirtliff. 2011. *Staphylococcus aureus* biofilms: Properties, regulation and roles in human disease. Virulence, **2**:445–459.

Baba, T., and O. Schneewind. 1998. Targeting of muralytic enzymes to the cell division site of Gram-positive bacteria: repeat domains direct autolysin to the equatorial surface ring of *Staphylococcus aureus*. The EMBO Journal, **17**:4639–4646.

Bharti, S.K., and R. Roy. 2012. Quantitative H NMR spectroscopy. Trends in Analytical Chemistry, **35:**5–26.

Beck, W. D., B. Berger-Bächi, and F. H. Kayser. 1986. Additional DNA in methicillin-resistant Staphylococcus aureus and molecular cloning of mec-specific DNA. Journal of Bacteriology, **165**:373–378.

Bera, A., S. Herbert, A. Jakob, W. Vollmer, and F. Götz. 2005. Why are pathogenic staphylococci so lysozyme resistant? The peptidoglycan O-acetyltransferase OatA is the major determinant for lysozyme resistance of *Staphylococcus aureus*. Molecular Microbiology, **55**:778–787.

Berger-Bächi B., A. Strassle, J. E. Gustafson, and F. H. Kayser. 1992. Mapping and characterization of multiple chromosomal factors involved in methicillin resistance in *Staphylococcus aureus*. Antimicrobial Agents and Chemotherapy, **36**:1367-1373.

Bergey, D. H., Robert Earle Buchanan, and N. E. Gibbons. 1974. Bergey's manual of determinative bacteriology. 8th ed Williams & Wilkins. Baltimore.

Biswas, R., L. Voggu, U. K. Simon, P. Hentschel, G. Thumm, and F. Götz. 2006. Activity of the major staphylococcal autolysin Atl. FEMS Microbiology Letters, **259**:260-268.

Boles, B. R., M. Thoendel, A. J. Roth, and A.R. Horswill. 2010. Identification of genes involved in polysaccharide-independent *Staphylococcus aureus* biofilm formation. PLoS One, **5**:e10146.

Bose, J. L., M. K. Lehman, P. D. Fey, and W.K. Bayles. 2012. Contribution of the *Staphylococcus aureus* Atl AM and GL murein hydrolase activities in cell division, autolysis and biofilm formation. Plos One, **7**:e42244.

Boucher, H., L. G. Miller, and R.R. Razonable. 2010. Serious infections caused by methicillin-resistant *Staphylococcus aureus*. Clinical Infectious Diseases, **51**:183–197.

Chambers, H. F. 2001. The changing epidemiology of *Staphylococcus aureus*? Emerging Infectious Diseases Journal, **7**:178–182.

Chambers H. F., and F. R. DeLeo. 2009. Waves of resistance: *Staphylococcus aureus* in the antibiotic era. Nature Reviews Microbiology, **7**:629-641.

Couto, I., H. de Lencastre, E. Severina, W. Kloos, J. A. Webster, R. J. Hubner, I. S. Sanches, and A. Tomasz. 1996. Ubiquitous presence of a *mecA* homologue in natural isolates of *Staphylococcus sciuri.* Microbial Drug Resistance, **2**:377-391.

Das, T., P. K. Sharma, H. J. Busscher, H. C. van der Mei, and B. P. Krom. 2010. Role of extracellular DNA in initial bacterial adhesion and surface aggregation. Applied Environmental Microbiology, **76**:3405-3408.

David, M. Z., and R. S Daum. 2010. Community-associated methicillin-resistant *Staphylococcus aureus*: epidemiology and clinical consequences of an emerging epidemic. Clinical Microbiology Reviews, **23**:616-687.

de Lencastre, H., S. W. Wu, M. G. Pinho, A. M. Ludovice, S. Filipe, S. Gardete, R. Sobral, S. Gill, M. Chung and, A. Tomasz. 1999. Antibiotic resistance as a stress response: complete sequencing of a large number of chromosomal loci in

Staphylococcus aureus strain COL that impact on the expression of resistance to methicillin. Microbial Drug Resistance, **5**:163-175.

DeLeo F. R., M. Otto, B. N. Kreiswirth, and H. F. Chambers. 2010. Community-associated methicillin-resistant *Staphylococcus aureus*. The Lancet, **375**:1557-1568.

Edwards A. M., R. C. Massey, and S. R. Clarke. 2012. Molecular mechanisms of *Staphylococcus aureus* nasopharyngeal colonization. Molecular Oral Microbiology, **27**:1-10.

Ehlert, K., and J. V. Holtje. 1996. Role of precursor translocation in coordination of murein and phospholipid synthesis in *E.coli*. Journal of Bacteriology, **178**:6766-6771.

Figueiredo T.A., R. G. Sobral, A. M. Ludovice, J. M. Almeida, N. K. Bui, W. Vollmer, H. de Lencastre, and A. Tomasz. 2012. Identification of genetic determinants and enzymes involved with the amidation of glutamic acid residues in the peptidoglycan of Staphylococcus aureus. PLoS Pathogens **8**:e1002508.

Foster, T. J. 2005. Immune evasion by staphylococci. Nature Reviews Microbiology, **3**:948–958.

Ghuysen, J. M. 1991. Serine β-Lactamases and Penicillin-Binding Proteins. Annual Review of Microbiology, **45**:37-67.

Giesbrecht, P., J. Wecke, and B. Reinicke. 1976. On themorphogenesis of the cell wall of staphylococci. Internation Review of Cytology, **44**:225–318.

Goffin, C., and J. M. Ghuysen. 1998. Multimodular penicillin-binding proteins: an enigmatic family of orthologs and paralogs. Microbiology and Molecular Biology Reviews, **62**:1079-1093.

Götz, F., C. Heilmann, T. Stehle. 2014. Functional and structural analysis of the major amidase (Atl) in *Staphylococcus*. International Journal of Medical Microbiology, **304:**156-163.

Grilo, I., A. M. Ludovice, A. Tomasz, H. de Lencastre, and R. Sobral. 2014. The glucosaminidase domain of Atl – the major *Staphylococcus aureus* autolysin – has DNA-binding activity. Microbiology Open, **3**:247-256.

Hartman, B. and A. Tomasz. 1984. Low-Affinity Penicillin-Binding Protein Associated with β-Lactam Resistance in *Staphylococcus aureus*. Journal of bacteriology, **158**:513-516.

Heilmann C., C. Gerke, F. Perdreau-Remington, and F. Götz. 1996. Characterization of Tn917 insertion mutants of *Staphylococcus epidermidis* affected in biofilm formation. Infection and Immunity, **64**:277–282.

Heilmann, C., J. Hartleib, M. S. Hussain, and G. Peters. 2005. The multifunctional *Staphylococcus aureus* autolysin aaa mediates adherence to immobilized fibrinogen and fibronectin. Infection and Immunity, **73**:4793-4802.

Heilmann, C., M. Hussain, G. Peters, and F. Götz. 1997. Evidence for autolysin-mediated primary attachment of *Staphylococcus epidermidis* to a polystyrene surface. Molecular Microbiology, **24**:1013–1024.

Hell, W., H. G. Meyer, and S. G. Gatermann. 1998. Cloning of aas, a gene encoding a *Staphylococcus saprophyticus* surface protein with adhesive and autolytic properties. Molecular Microbiology, **29**:871–881.

Holtje, J. V. 1998. Growth of the stress-bearing and shape-maintaining murein sacculus of *E. coli*. Microbiology and Molecular Biology Reviews, **62**:181-203.

Houston, P., S. E. Rowe, C. Pozzi, E. M. Waters, and J. P. O'Gara. 2011. Essential Role for the Major Autolysin in the Fibronectin-Binding Protein-Mediated *Staphylococcus aureus* Biofilm Phenotype . Infection and Immunity. **79**:1153–1165.

Iwase, T., H. Shinji, A. Tajima, F. Sato, T. Tamura, T. Iwamoto, M. Yoneda, and Y. Mizunoe. 2010. Isolation and Identification of ATP-Secreting Bacteria from Mice and Humans. Journal of Clinical Microbiology, **48**:1949–1951.

Jevons, P. 1961. “Celbenin”-resistant Staphylococci. British Medical Journal **1**:124-125.

Johnson, A. P., A. Pearson, and G. Duckworth. 2005. Survaillance and epidemiology of MRSA bacteraemia in the UK. Journal of Antimicrobial Chemotherapy, **56**:455-462.

Jordan, S., M. Hutchings, and T. Mascher. 2007. Cell envelope stress response in Gram-positive bacteria. FEMS Microbiology, **32**:107-146.

Kaplan, J. B., E. A., Izano, P. Gopal, M. T. Karwacki, S. Kim, J. L. Bose, and A.R. Horswill. 2012. Low Levels of β-Lactam Antibiotics Induce Extracellular DNA Release and Biofilm Formation in *Staphylococcus aureus*. mBio, **3**:e00198–12.

Kloos, W. E. 1997. Taxonomy and systematics of staphylococci indigenous to humans. pp. 113–117. *In* Crossley B., Archer G. L., editors. The staphylococci in human disease. N.Y: Churchill Livingstone. New York.

Kluytmans, J., A. van Belkum, and H. Verbrugh. 1997. Nasal carriage of *Staphylococcus aureus*: epidemiology, underlying mechanisms, and associated risks. Clinical Microbiology Reviews, **10**:505–520.

Lee, J. H. 2003. Methicillin (Oxacillin)-resistant *Staphylococcus aureus* strains isolated from major food animals and their potential transmission to humans. Applied Environmental Microbiology, **69**:6489-6494.

Lee, S. H., L. W. Jarantow, H. Wang, S. Sillaots, H. Cheng, T. C. Meredith, J. Thompson, and T. Roemer. 2011. Antagonism of chemical genetic interaction networks resensitize MRSA to β-lactam antibiotics. Chemistry & Biology, **18**:1379–1389.

Levy, O. 2000. Review article Antimicrobial proteins and peptides of blood : templates for novel antimicrobial agents. Blood, **96**:2664-2672.

Mann, E. E., K. C. Rice, B. R. Boles, J. L. Endres, D. Ranjit, L. Chandramohan, and K.W. Bayles. 2009. Modulation of eDNA Release and Degradation Affects *Staphylococcus aureus* Biofilm Maturation. PLoS one, **4**:e5822.

Marino, M., M. Banerjee, R. Jonquières, P. Cossart, and P. Ghosh. 2002. GW domains of the *Listeria monocytogenes* invasion protein InlB are SH3-like and mediate binding to host ligands. The EMBO Journal, **21**:5623–5634.

Mediavilla, J.R., L. Chen, B. Mathema, and B.N. Kreiswirth. 2012. Global epidemiology of community-associated methicillin resistant *Staphyloccus aureus* (CA-MRSA). Current Opinion in Microbiology, **15:**588-595.

Moellering, R.C. Jr. 2012. MRSA: the first half century. Journal of Antimicrobial Chemotherapy, **67:**4-11.

Monecke, S., G. Coombs, A.C. Shore, D.C. Coleman, P. Akpaka, M. Borg, H. Chow, M.Ip, L. Latzwauk, D. Jonas, K. Kadleck, A. Kearns, F. Laurent, F.G. O'Brien, J. Pearson, A. Ruppelt, S.Schwarz, E. Scicluna, P. Slickers, H.L. Tan, S. Weber, and R. Ehricht. 2011. A field guide to pandemic, epidemic and sporadic clones of methicillin-resistant *Staphylococcus aureus*. PLoS One, **6**:e17936.

Montelione, G.T., D. Zheng, Y.J. Huang, K.C. Gunsalus, and T. Szyperski. 2000. Protein NMR spectroscopy in structural genomics. Nature Structural & Molecular Biology, **7**:982-985.

Nair, N., V. Vinod, M. Suresh, S. Vijayrajratnam, L. Biswas, R. Peethambaran, A.K. Vasudevan, R. Biswas. 2015. Amidase, a cell wall hydrolase, elicits protective immunity against *Staphylococcus aureus* and *S. epidermidis*. International Journal of Biological Macromolecules, **77**:314-321.

Nanninga, N. 1998. Morphogenesis of *E.coli*. Microbiology and Molecular Biology Reviews, **62**:110-129.

Oliveira, D.C., A. Tomasz, and H. de Lencastre. 2002. Secrets of success of a human pathogen: molecular evolution of pandemic clones of meticillin-resistant *Staphylococcus aureus.* The Lancet Infectious Diseases, **2**:180-189.

Oshida, T., M. Sugai, H. Komatsuzawa, Y. M. Hong, H. Suginaka, and A. Tomasz. 1995. A *Staphylococcus aureus* autolysin that has an N-acetylmuramoyl-L-alanine amidase domain and an endo-beta-N-acetylglucosaminidase domain: cloning, sequence

analysis, and characterization. Proceedings of the National Academy of Sciences of the United States of America, **92**:285–289.

Otto, M. 2012. MRSA virulence and spread. Cellular Microbiology, **14**:1513-1521.

Pfaller, M., E.D. Davenport, M. Bale, M. Barrett, F. Koontz, and R.M. Massanari. 1988. Development of the quantitative microtest for slime production by coagulase-negative staphylococci. European Journal of Clinical Microbiology **7**:30-3.

Plata, K., A. E. Rosato, and G. Wegrzyn. 2009. *Staphylococcus aureus* as an infectious agent: overview of biochemistry and molecular genetics of its pathogenicity. Acta Biochimica Polonica, **56**:597-612.

Projan, S. J., and R. P. Novick. 1997. The molecular basis of pathogenicity, p. 55-81. *In* K. B. Crossley and G. L. Archer (ed.), The staphylococci in human disease. Churchill Livingstone Inc., New York.

Ramadurai, L., and R. K. Jayaswal. 1997. Molecular cloning, sequencing, and expression of lytM, a unique autolytic gene of *Staphylococcus aureus*. Journal of Bacteriology, **179**:3625-3631.

Ramadurai, L., K. J. Lockwood, M. J. Nadakavukaren, and R. K. Jayaswal. 1999. Characterization of a chromosomally encoded glycyglycine endopeptidase of *Staphylococcus aureus.* Microbiology, **145**:801-808.

Reichmann, N. T., and A. Grundling. 2011. Location, synthesis and function of glycolipids and polyglycerolphosphate lipoteichoic acid in Gram-positive bacteria of the phylum Firmicutes. FEMS Microbiology Letters, **319**:97–105.

Reynolds, P. E., and D. F. Brown. 1985. Penicillin-binding proteins of beta-lactam-resistant strains of *Staphylococcus aureus*. Effect of growth conditions. FEBS Letters, **192**:28–32.

Rice, K. C., E. E. Mann, J. L. Endres, E. C. Weiss, J. E. Cassat, M. S. Smeltzer, and K. W. Bayles. 2007. The *cidA* murein hydrolase regulator contributes to DNA release and biofilm development in *Staphylococcus aureus*. Proceedings of the National Academy of Sciences of the United States of America, **104**:8113–8118.

Roemer, T., T. Schneider, and M. G. Pinho. 2013. Auxiliary factors: a chink in the armor of MRSA resistance to β-lactam antibiotics. Current Opinion in Microbiology, **16**:538-548.

Rolo, J., H. de Lencastre, and M. Miragaia. 2013. High frequency and diversity of cassette chromosome recombinases (ccr) in methicillin-susceptible *Staphylococcus sciuri*. Journal of Antimicrobial Chemotherapy, **69**:1461–1469.

Sadykov, M. R., and K.W. Bayles. 2012. The control of death and lysis in staphylococcal biofilms: a coordination of physiological signals. Current Opinion in Microbiology, **15**:211–215.

Schindler, M., Y. Assaf, N. Sharon, and D. M. Chipman. 1997. Mechanism of lysozyme catalysis: Role of ground-state strain in subsite D in hen egg-white and human lysozymes. Biochemistry, **16**:423-431.

Schleifer, K. H., and O. Kandler. 1972 Peptidoglycan types of bacterial cell walls and their taxonomic implications. Bacteriological Reviews, **36**:407-477.

Seybold U., E.V. Kourbatova, J.G. Johnson, S.J. Halvosa, Y.F. Wang, M.D. King, S.M. Ray, and H.M. Blumberg. 2006. Emergence of community-associated methicillin-resistant *Staphylococcus aureus* USA 300 genotype as a major cause of health care– associated blood stream infections. Clinical Infectious Diseases, **42**:647–466.

Schlag, M., R. Biswas, B. Krismer,T. Kohler, S. Zoll,W. Yu, H. Scwarz, A. Peschel, and F. Götz. 2010. Role of staphylococcal wall teichoic acid in targeting the major autolysin Atl. Molecular Microbiology, **75**:864-873.

Shore, A. C., E. C. Deasy, P. Slickers, G. Brennan, B. O'Connell, S. Monecke, R. Ehricht, and D. C. Coleman. 2011. Detection of staphylococcal cassette chromosome *mec* type XI carrying highly divergent *mecA, mecI, mecR1, blaZ* and *ccr* genes in human clinical isolates of clonal complex130 methicillin-resistant *Staphylococcus aureus*. Antimicrobial Agents and Chemotherapy, **55**:3765-3773.

Smith, C. A. 2006. Structure, function and dynamics in the mur family of bacterial cell wall ligases. Journal of Molecular Biology, **362**:640-655.

Studier, F. W. 2005. Protein Production by Auto-Induction in High-Density Shaking Cultures. Protein Expression and Purification, **41**:207–234.

Sugai, M., S. Yamada, S. Nakashima, H. Komatsuzawa, A. Matsumoto, T. Oshida, and H. Suginaka. 1997. Localized perforation of the cell wall by a major autolysin: atl gene products and the onset of penicillin-induced lysis of *Staphylococcus aureus*. Journal of Bacteriology, **179**:2958–2962.

Szweda P., M. Schielmann, R. Kotlowski, G. Gorczyca, M. Zalewska, and S. Milewski. 2012. Peptidoglycan hydrolases-potential weapons against *Staphylococcus aureus.* Applied Microbiology and Biotechnology, **96**:1157-1174.

Tomasz, A., and H. de Lencastre. 1997. Molecular microbiology and epidemiology: coexistance or alliance? P. 309-321. *In* R.P. Wenzel (ed) Prevention and control of nosocomial infections. Williams & Wilkins, Baltimore, MD, USA.

Tzagoloff, H., and R. Novick. 1977. Geometry of cell division in *Staphylococcus aureus.* Journal of Bacteriology, **129**:343–350.

Uhlemann, A.C., S. F. Porcella, S. Trivedi, S. B. Sullivan, C. Hafer, A. D. Kennedy, and F.D. Lowy. 2012. Identification of a Highly Transmissible Animal-Independent *Staphylococcus aureus* ST398 Clone with Distinct Genomic and Cell Adhesion Properties. mBio, **3**:e00027–12.

Van Bambeke, F., D. M. Lambert, M. P. Mingeot-Leclercq, and P.M. Tulkens. 2003. Anti-infective therapy: Mechanism of action. 7.1.1-7.1.14. *In* Armstrong, J Cohen (ed.), Infectious Diseases. London, United Kingdom.

van Heijenoort, J. 2007. Lipid intermediates in the biosynthesis of bacterial peptidoglycan. Microbiology and Molecular Biology Reviews, **71**:620-635.

Vollmer W., D. Blanot, and M. A. de Pedro. 2008. Peptidoglycan structure and architecture. FEMS Microbiology Reviews, **32**:149-167.

Watkins R. R., M. Z. David, and R.A. Salata. 2012. Current concepts on the virulence mechanisms of methicillin-resistant *Staphylococcus aureus.* Journal of Medical Microbiology, **61**:1179-1193.

Xia, G., T. Kohler, and A. Peschel. 2010a. The wall teichoic acid and lipoteichoic acid polymers of *Staphylococcus aureus*. International Journal of Medical Microbiology, **300**:148–154.

Yamada, S., M. Sugai, H. Komatsuzawa, S. Nakashima, T. Oshida, A. Matsumoto, and H. Suginaka. 1996. An autolysin ring associated with cell separation of *Staphylococcus aureus*. Journal of Bacteriology, **178**:1565–1571.

Zhou, X., and L. Cegelski. 2012. Nutrient-dependent Structural Changes in *S. aureus* Peptidoglycan Revealed by Solid-State NMR Spectroscopy. Biochemistry, **51**:8143–8153.

Zoll, S., B. Pätzold, M. Schlag, F. Götz, H. Kalbacher, and T. Stehle. 2010. Structural Basis of Cell Wall Cleavage by a Staphylococcal Autolysin. PLoS Pathogens, **6**:e1.

Annex

1. Impact of the GL-DNA association in biofilm formation. (Grilo *et al*, 2014)

It has been shown that *atl* mutants do not form biofilm presumably due to the role of the autolysin in genomic DNA release and also in assisting the attachment of cells to the surface during the first phases of biofilm formation.

1.1. Involvement of ATL in biofilm formation of strain MW2

These preliminary studies tested the independent and combined roles of AM and GL domains in biofilm formation, using a *S. aureus* strain, MW2, that form biofilm.

In order to understand biofilm forming capacity of the *atl* mutant, an assay with different recombinant ATL proteins was performed. (Figure 18)

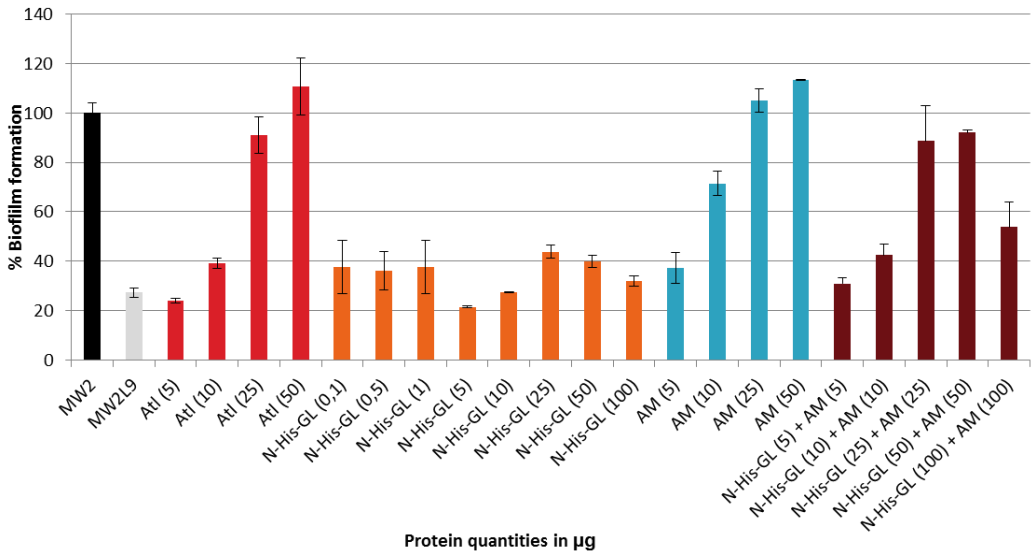

Figure 18 – Biofilm formation of strain MW2, its isogenic *atl* mutant MW2L9, and MW2L9 with added recombinant proteins. Atl refers to the $AMR_{1\text{-}3}GL$ recombinant protein, N-His-GL refers to R_3GL, and AM refers to $AMR_{1\text{-}2}$. Three experiments were performed, at least in duplicates.

Protein $AMR_{1\text{-}2}$ was able to complement the biofilm forming capacity of the mutant, owing to the increase of extracellular DNA present in the media due to the lytic activity of the added recombinant protein. When $AMR_{1\text{-}2}$ and R_3GL proteins were added together, as well the complete protein $AMR_{1\text{-}3}GL$, the biofilm forming capacity was also complemented, although only for higher protein amounts. However, when R_3GL

was added alone no complementation of biofilm formation occurred. In some cases, the biofilm forming capacity of the mutant with R_3GL was lower than the mutant alone, and no concentration dependence was seen.

1.2. Involvement of ATL in biofilm formation in different strains.

To analyze the importance of ATL in biofilm formation strains were chosen due to their high biofilm forming capacity and *atl* mutants were obtain (by transduction of the RUSAL9 transposition mutant with phage 80α). The resulting isogenic *atl* mutants were tested by Western Blot. Different patterns and amounts of GL protein were found between the different strains as shown at Figure 19.

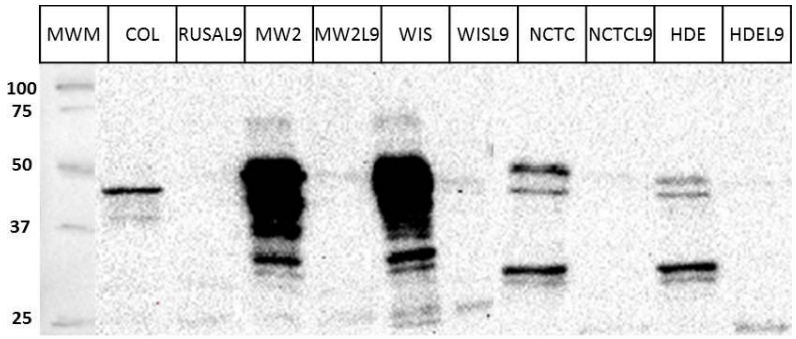

Figure 19 – Detection of GL protein performed by Western Blot using anti-GL raised antibody against cellular extracts of different strains and their respective isogenic *atl* mutants.

When static biofilm assays were performed on these strains and their *atl* mutants, only MW2L9 and WISL9 showed a decrease in biofilm formation when compared to the respective parental strains (Figure 20).

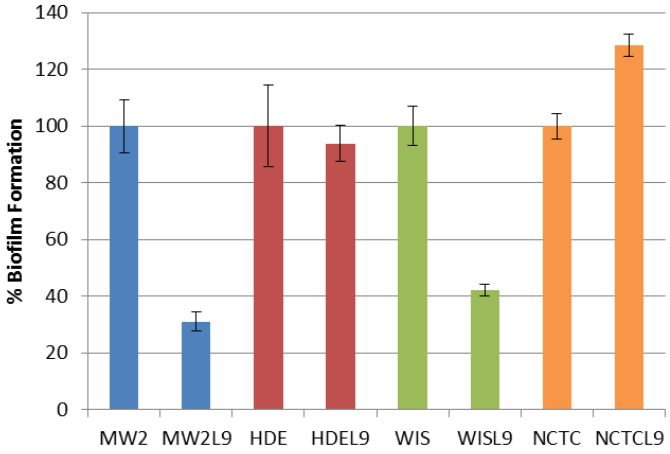

Figure 20 – Biofilm formation by strains MW2, HDE 288, WIS and NCTC 8325 and their respective isogenic *atl* mutants. Values shown are average values referring to the percentage of biofilm when compared to MW2 strain. Two experiments were performed, at least in triplicates.

These results were unexpected; the lack of *atl* is expected to result in a decrease in biofilm formation in *S. aureus*. However, this supports the importance of the genetic background on biofilm formation, and the different patterns found in the GL Western Blot could also justify the different impact that the lack of ATL has in biofilm formation, which is strain-dependent.

Also, the strains without *atl* has a diminished biofilm (MW2 and WIS) and similar Western patterns, with many smaller bands perhaps corresponding to extensive processing of GL protein.

1.3. Involvement of GL in biofilm formation in strain WIS

To study the biofilm forming capacity of strain WIS and its *atl* mutant, different ATL recombinant proteins in different concentrations were added. The biofilm forming capacity of strain WIS was progressively restored, achieving full complementation at a protein concentration of 10 µg. The addition of AMR1-2 and R3GL recombinant proteins together showed a higher biofilm forming capacity when compared to the addition of only one of these proteins, suggesting that the two proteins may work synergistically in promoting biofilm formation. (Figure 21)

Other variations were observed between WIS and MW2, showing that the different genetic background may be involved.

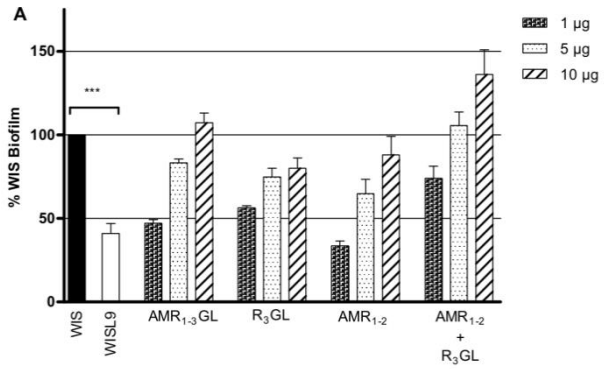

Figure 21 - Biofilm formation of *S. aureus* strain WIS and its isogenic *atl* mutant WISL9 with added recombinant proteins. Biofilms were grown with different amounts of extracellularly added recombinant GL domain (R3GL), AM domain (AMR1-2), and entire Atl recombinant protein lacking the SP and PP sequences (AMR1-3GL).

1.3.1. ATL-DNA association

The addition of extracellular DNA was able to complete the partial complementation achieved when added a less protein concentration (5 µg), however, full restoration was not achieved until AMR_{1-2} was added. This is consistent with a critical role for extracellular DNA in the GL-dependent biofilm formation process. (Figure 22)

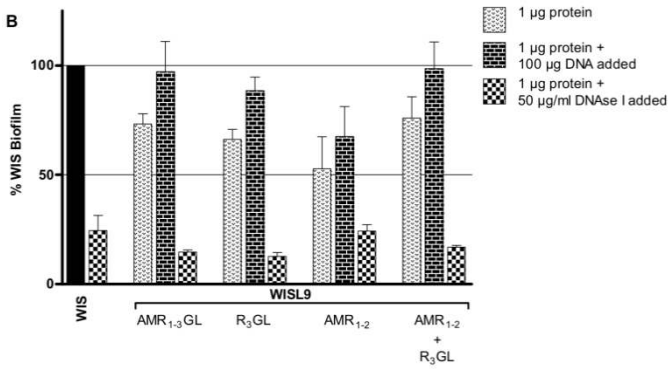

Figure 22 - Biofilm formation of *S. aureus* strain WIS and its isogenic *atl* mutant WISL9 with added recombinant proteins. Biofilms were grown with 1 µg of the different recombinant proteins and complemented with 100 µg of low molecular weight salmon sperm DNA or 50 µg/ml of DNase I.

Addition of complementing amounts of any of the recombinant proteins together with DNase I to the mutant resulted in an almost complete block of biofilm formation

(Figure 23). This effect was less distinct when only AMR1-2 was added, supporting the suggestion that the GL domain of ATL plays a more important role than the AM domain of this protein in the DNA-dependent formation of biofilm.

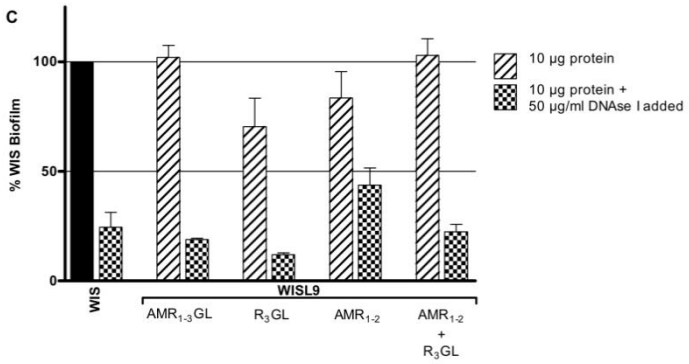

Figure 23 - Biofilm formation of *S. aureus* strain WIS and its isogenic *atl* mutant WISL9 with added recombinant proteins. Biofilms were grown with 10 µg of the different recombinant proteins, and addition of DNase I at 50 µg/ml disrupted biofilm formation. The amount of biofilm produced was calculated as a percentage of the biofilm produced by the parental WIS strain.

2. Lysis assay

The results obtained in the lysis assay of peptidoglycan are shown in the next graphics (Figure 24), there are no relevant differences in the lytic activity of GL when DNA is added.

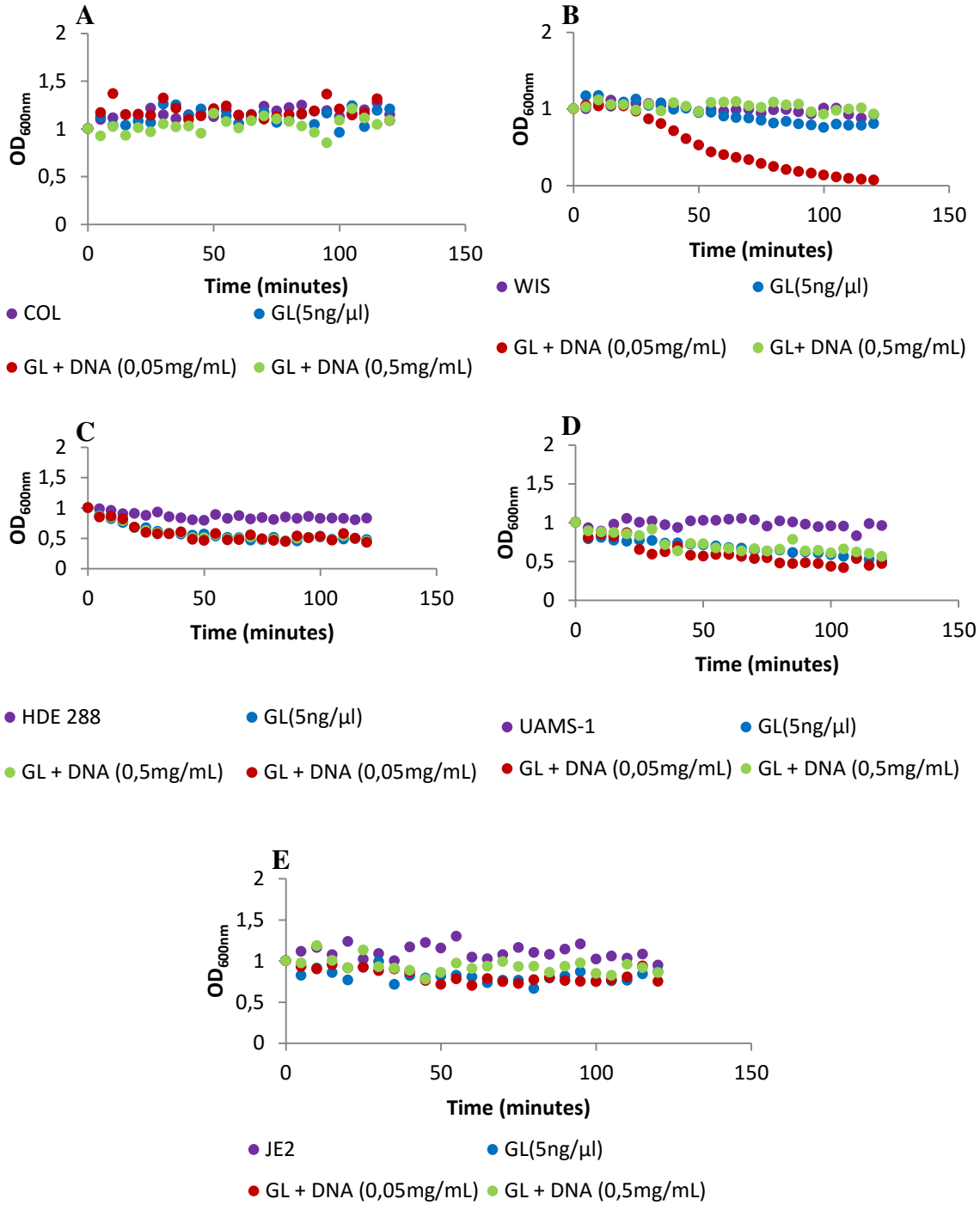

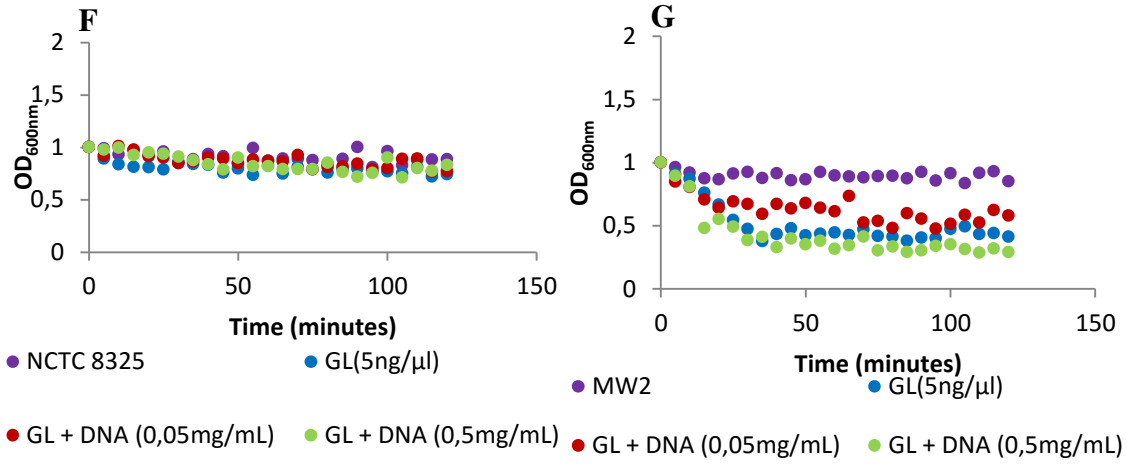

Figure 24 – Lytic activity of GL protein in peptidoglycan and DNA-GL association in different strains. (A) COL; (B) WIS; (C) HDE288; (D) UAMS-1; (E) JE2 (F) NCTC8325; (G) MW2. Purple: peptidoglycan without GL; Blue: peptidoglycan with GL 5ng/µl; Red: peptidoglycan with GL 5ng/µl and DNA(0,05mg/mL); Green: peptidoglycan with GL 5ng/µl and DNA(0,5mg/mL).

The results obtained in the lysis assay of cell wall are shown in the next graphics (Figure 25), there are no relevant differences in the lytic activity of GL when DNA is added.

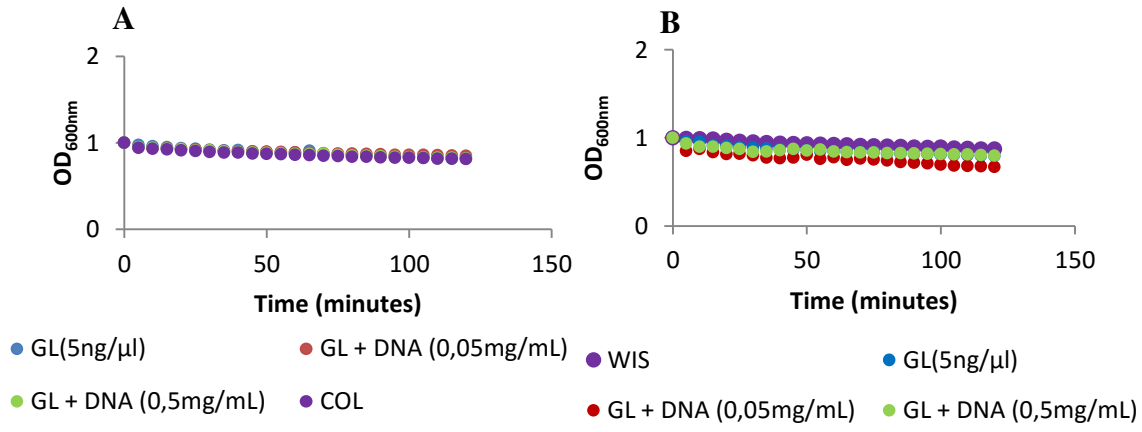

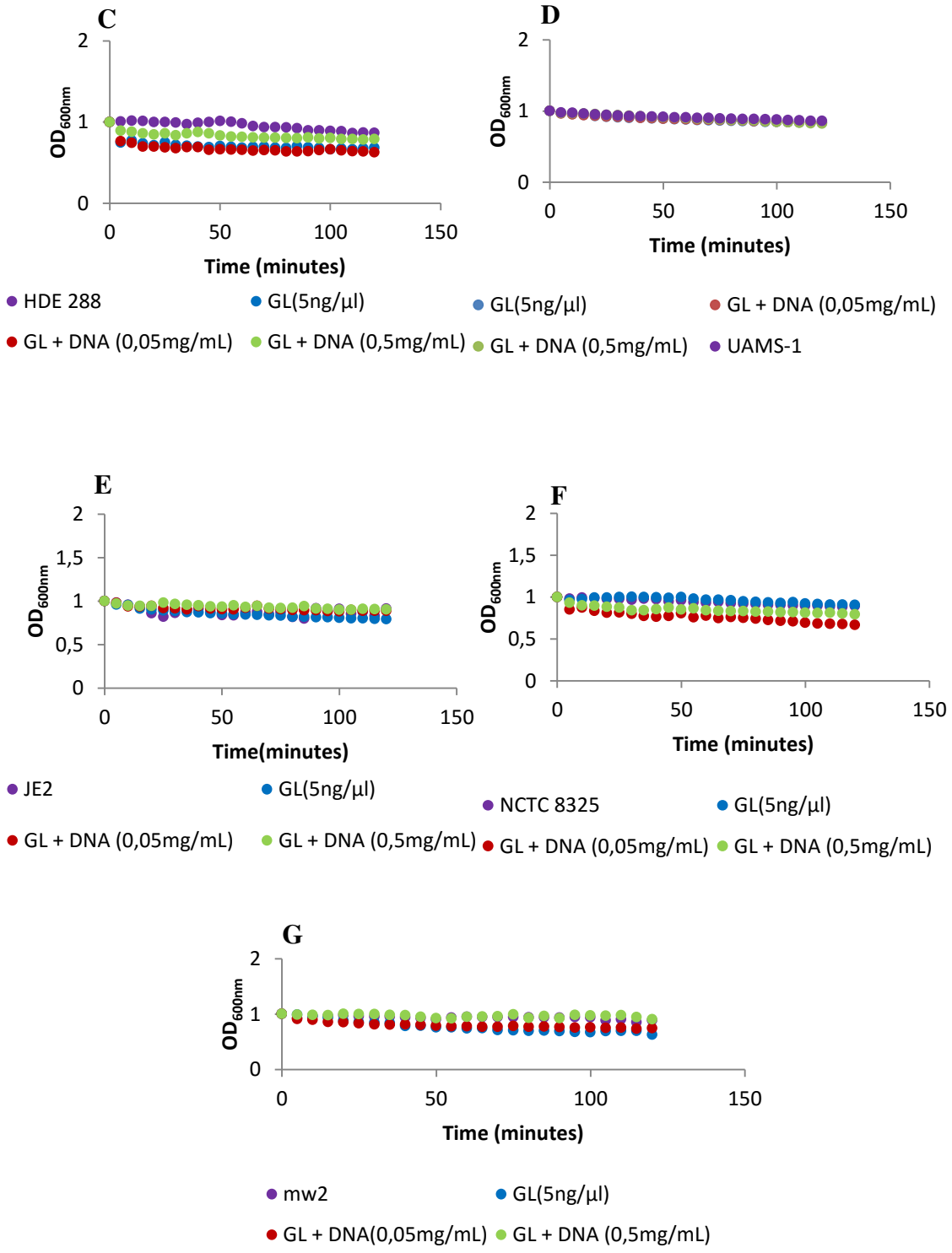

Figure 25- Lytic activity of GL protein in cell wall and DNA-GL association in different strains. (A) COL; (B) WIS; (C) HDE288; (D) UAMS-1; (E) JE2 (F) NCTC8325; (G) MW2. Purple: peptidoglycan without GL; Blue: peptidoglycan with GL 5ng/µl; Red: peptidoglycan with GL 5ng/µl and DNA(0,05mg/mL); Green: peptidoglycan with GL 5ng/µl and DNA(0,5mg/mL).

The results obtained in the heat inactivated cells lytic assay are shown in the next graphics (Figure 26).

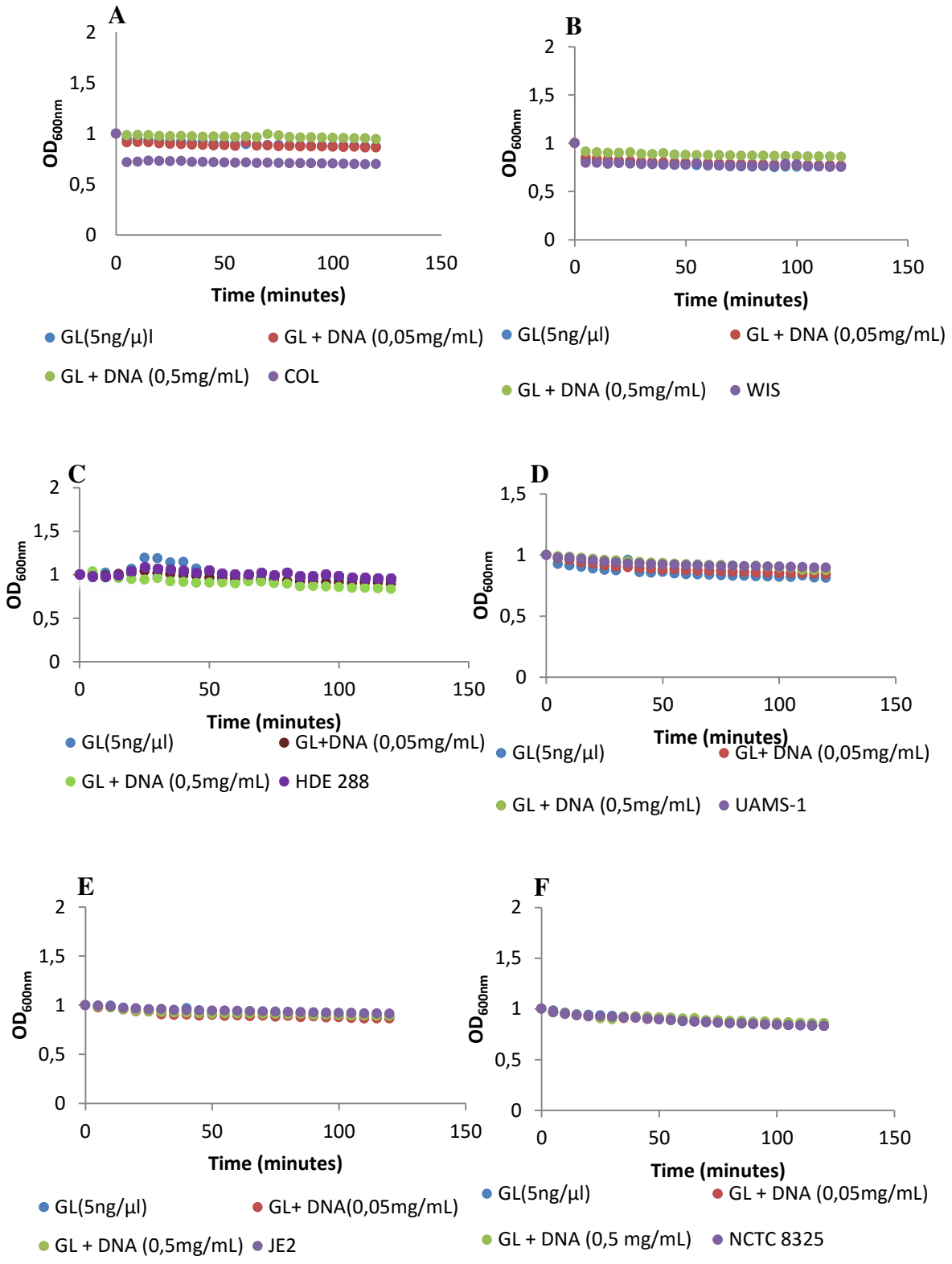

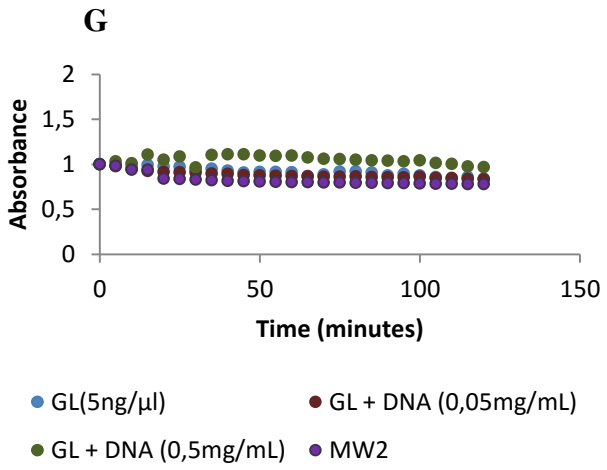

Figure 26- Lytic activity of GL protein in heat-inactivated cells and DNA-GL association in different strains. (A) COL; (B) WIS; (C) HDE288; (D) UAMS-1; (E) JE2 (F) NCTC8325; (G) MW2. Purple: peptidoglycan without GL; Blue: peptidoglycan with GL 5ng/µl; Red: peptidoglycan with GL 5ng/µl and DNA(0,05mg/mL); Green: peptidoglycan with GL 5ng/µl and DNA(0,5mg/mL).

3. Stock solutions

3.1. 20xNPS (1 litre)

Solution	m (g)
0.5M $(NH_4)_2SO_4$	66 g
1M KH_2PO_4	136 g
1M Na_2HPO_4	142 g
dd H_2O	900 ml

3.2. Trace metals

Solution	MM (g/mol)	m (g)	Volume (mL)	1000x final volume (µL)	1000x Final concentration (mM)
1M $CaCl_2$	-	-	-	20	20
100 mM $MnCl_2$	197,91	0,1979	10	100	10
20 mM H_3BO_3	61,3	0,12366	10	100	2
20mM Na_2MoO_4 ($2H_2O$)	241,95	0,04839	10	100	2
20 mM $CoCl_2$ ($6H_2O$)	237,93	0,04759	10	100	2
20 mM $CuCl_2$ ($2H_2O$)	170,48	0,034096	10	100	2
20 mM $NiCl_2$ ($6H_2O$)	237,69	0,04754	10	100	2
20 mM Na_2SeO_3	263,01	0,052602	10	100	2
20 mM $ZnSO_4$	287,54	0,05751	10	100	2
0,5 M $FeCl_3$ [1] ($6H_2O$)	270,30	1,3515	10	100	50
dd H_2O	-	-	-	80	-

[1] Dissolve in HCl (diluted 1/100)